Magnetic fluid bearings & seals

Methods, design & application

Lampaert, S.G.E.

DOI
10.4233/uuid:361ba18e-298a-483c-bfb9-0528a4ee6119

Publication date
2020

Document Version
Final published version

Citation (APA)
Lampaert, S. G. E. (2020). *Magnetic fluid bearings & seals: Methods, design & application*. [Dissertation (TU Delft), Delft University of Technology]. https://doi.org/10.4233/uuid:361ba18e-298a-483c-bfb9-0528a4ee6119

Important note
To cite this publication, please use the final published version (if applicable).
Please check the document version above.

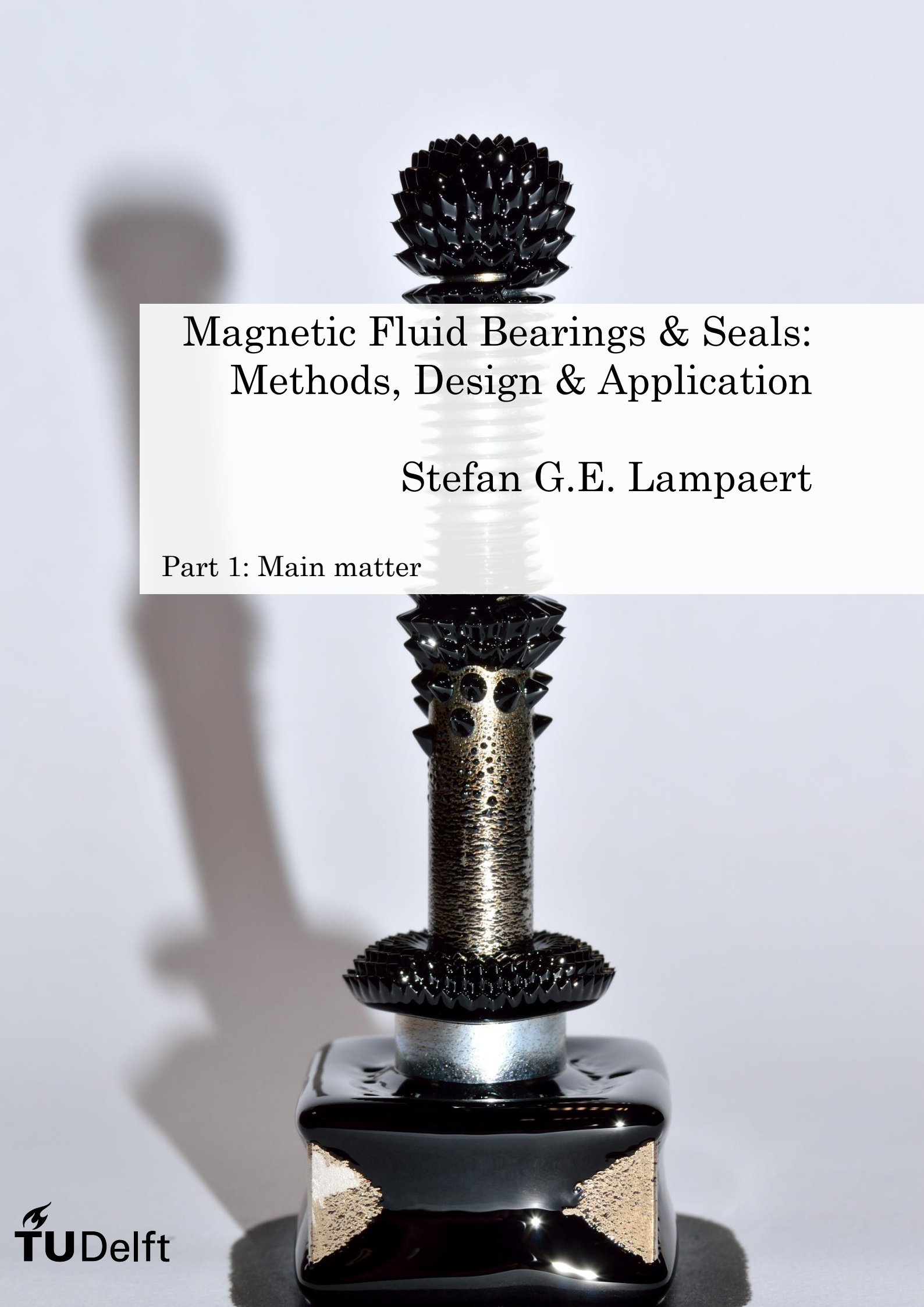

Magnetic Fluid Bearings & Seals: Methods, Design & Application

Stefan G.E. Lampaert

Part 1: Main matter

TU Delft

Magnetic Fluid Bearings & Seals: Methods, Design & Application

Dissertation

for the purpose of obtaining the degree of doctor
at Delft University of Technology
by the authority of the Rector Magnificus Prof.dr.ir. T.H.J.J. van der Hagen,
Chair of the Board for Doctorates
to be defended publicly on
Wednesday 30 September 2020 at 15:00 o'clock

by

Stefan Georges Emile LAMPAERT

Master of Science in Mechanical Engineering,
Delft University of Technology, The Netherlands
born in Terneuzen, The Netherlands

This dissertation has been approved by the promotor[s].

Composition of the doctoral committee:

Rector Magnificus,	chairperson
Dr.ir. R.A.J. van Ostayen	Delft University of Technology, promotor
Ir. J.W. Spronck	Delft University of Technology, copromotor

Independent members:

Prof.dr. P.C. Rem	Delft University of Technology
Prof.dr. I. Sherrington	University of Central Lancashire
Prof.dr.-ing. I.F. Santos	Technical University of Denmark
Prof.dr.ir. M.B. de Rooij	University of Twente
Prof.dr.ir. J.L. Herder	Delft University of Technology

Keywords: ferrofluid, magnetorheological fluids, rheology, lubrication theory, self-healing, load capacity, stiffness, friction, hydrodynamic bearing, hydrostatic bearing.
Published by: TU Delft Library
Printed by: Gildeprint Enschede

Email: stefan@lampaert.nl
ISBN: 9789464190427
An electronic copy of this dissertation is available at the TU Delft Repository

"He achieved success who has lived well, laughed often, and loved much;
Who has enjoyed the trust of pure women, the respect of intelligent men and the love of little children;
Who has filled his niche and accomplished his task;
Who has never lacked appreciation of Earth's beauty or failed to express it;
Who has left the world better than he found it,
Whether an improved poppy, a perfect poem, or a rescued soul;
Who has always looked for the best in others and given them the best he had;
Whose life was an inspiration;
Whose memory a benediction. "

Bessie Anderson Stanley, 1904, What is success?

Table of contents

Summary

The bearing and the seal are two commonly used tribological components since nearly all moving machinery relies on them for proper operation. Even a small improvement in these components can have a big impact on both the market and the environment. The two main problems of these components are wear and friction. In addition, seals suffer from the problem of leakage which is fundamental to both their functioning as well as their performance.

The application of magnetic fluids has the potential to be beneficial for these systems. Magnetic fluids consist of a suspension of magnetic particles in a carrier fluid. This gives them the unique properties of being attracted to a magnetic field and changing their rheological behaviour in the presence of a magnetic field. These special properties can give these bearing and sealing systems unique behaviour, potentially improving their performance.

Therefore, this thesis has two main objectives. The first objective is to further investigate the potential of magnetic fluids in bearing and sealing system. This part consists of exploratory, fundamental and early stage research. The unique properties of magnetic fluids are eventually used in ferrofluid bearings, ferrofluid seals, bearings with rheological textures and self-healing bearings. The second objective is to develop the necessary knowledge to bring these concepts to society in the form of applications.

The research on ferrofluid bearings as described in this thesis consists of different experimentally validated models for the load capacity, torque capacity, out of plane stiffness, rotational stiffness, friction and operational range for both ferrofluid pocket bearings and ferrofluid pressure bearings. These models are suitable to determine the most important bearing parameters which makes it possible to design a bearing system according to desired specifications. The most recent demonstrator shows specifications that are competitive with conventional bearing systems.

The research on ferrofluid seals as described in this thesis has resulted in the first seal concept that does not show any leakage over time. The concept relies on a replenishment system that makes sure that that degraded ferrofluid is removed and replaced by fresh ferrofluid. This gives the system a theoretical infinite lifetime, as long as the replenishment system continues to work.

The research on bearings with magnetorheological fluids as described in this thesis has resulted in the new design concept of rheological textures. A rheological texture is defined to be a local change in the rheological behaviour of the lubricant in the lubricating film such that a local change in lubricant transport and flow resistance occurs. The idea is to replace geometrical surface textures of more traditional bearings with these rheological textures to enhance the performance of the bearing. This work has in addition provided a new lubrication theory for Bingham plastics that properly models the behaviour. Furthermore, a new

experimental method is developed to characterize the rheology of magnetic fluids at high shear rates.

The last significant result of this research is the new concept of a self-healing bearing using a lubricant with a suspension of magnetic particles: the application of a local magnetic field with high gradients in the lubricating film causes the particles to settle at locations where the magnetic field gradient is high. This creates geometrical surface textures that will regrow when worn away. In this way we have a bearing with a surface texture that has a theoretical infinite lifetime.

Samenvatting

De lager en de afdichting zijn twee veel gebruikte tribologische componenten doordat vrijwel alle bewegende machines op ze vertrouwen voor een juiste werking. Zelfs een kleine verbetering in deze componenten kan een grote impact hebben op zowel de markt als het milieu. De twee voornaamste problemen van deze componenten zijn slijtage en wrijving. Daar bovenop lijden afdichten onder het probleem van lekkage welke fundamenteel is voor zowel hun functioneren als hun prestaties.

De toepassing van magnetische vloeistoffen heeft de potentie om voordelig te zijn voor deze systemen. Magnetische vloeistoffen bestaan uit een suspensie van magnetische deeltjes en een drager vloeistof. Dit geeft ze de unieke eigenschap om aangetrokken te zijn door een magnetisch veld en om van reologisch gedrag te veranderen in reactie tot een magnetisch veld. Deze special eigenschappen kunnen lagers en afdichtingen uniek gedrag geven dat potentieel hun gedrag bevorderd.

Daarom heeft deze thesis twee hoofddoelen. Het eerste doel is om verder de potentie van magnetische vloeistoffen in lager en afdichtingsystemen te onderzoeken. Dit deel bestaat uit exploraties, fundamenteel en vroege fase onderzoek. De unieke eigenschappen van magnetische vloeistoffen zijn uiteindelijk gebruikt in ferrofluid lagers, ferrofluid afdichtingen, lagers met reologische texturen en zelf genezende lagers. Het tweede doel is om alle benodigde kennis te ontwikkelen om deze concepten naar de maatschappij te kunnen brengen in de vorm van applicaties.

Het onderzoek naar ferrofluid lagers zoals beschreven in deze thesis bestaat uit verschillende experimenteel gevalideerde modellen voor de draagkracht, momentcapaciteit, stijfheid uit het vlak, rationele stijfheid, wrijving en operationeel bereik voor zowel ferrofluid pocket lagers en ferrofluid druk lagers. Deze modellen zijn bruikbaar om de belangrijkste lager parameters vast te stellen welke het mogelijk maakt om een lager naar gewenste specificaties te ontwerpen. De meest recente demonstratie opstelling laat specificaties zien die vergelijkbaar zijn met conventionele lager systemen.

Het onderzoek naar ferrofluid afdichtingen zoals beschreven in deze thesis heeft geresulteerd in het eerste concept dat geen enkele vorm van lekkage vertoont over tijd. Het concept vertrouwd op een verversingsysteem dat ervoor zorgt dat de gedegradeerde ferrofluid wordt verwijderd en vervangen door verse ferrofluid. Dit geeft het systeem een theoretisch oneindige levensduur, zoals het verversingsysteem blijft werken.

Het onderzoek aan lagers met magnetorheologische vloeistoffen zoals beschreven in deze thesis heeft geresulteerd in het nieuwe concept van reologische texturen. Een reologische textuur is gedefinieerd als een lokale verandering in het reologische gedrag van het smeermiddel in de smeerfilm zodat een lokale verandering in smeermiddel transport en stroom weerstand ontstaat. Het idee is om geometrische texturen van traditionele lagers te vervangen

met deze reologische texturen zodat de prestaties van het lager verbeteren. Dit werk heeft ook een nieuwe smeringstheorie voor Bingham vloeistoffen opgeleverd welke het gedrag op een juiste manier beschrijft. Daarbovenop is een nieuwe experimentele methode ontwikkeld om de reologie van magnetische vloeistoffen te karakteriseren op hoge afschuifsnelheden.

Het laatste significante resultaat van dit onderzoek is het nieuwe concept van zelf genezende lagers gebruikmakend van een suspensie van magnetische deeltjes: de applicatie van een lokaal magnetisch veld met een hoog gradiënt in de smeringsfilm zorgt ervoor dat de deeltjes neerslaan op de locaties waar de veldsterkte hoog is. Dit creëert geometrische oppervlakte texturen die terugroeien als ze wegslijten. Op deze manier hebben we een lager met een oppervlakte textuur die een theoretisch oneindige levensduur heeft.

Prologue

"Innovation is more than having new ideas: it includes the process of successfully introducing them or making things happen in a new way. It turns ideas into useful, practicable and commercial products or services."

— John Adair, 2009

What does it mean to innovate? According to the Oxford dictionary it means to make changes in something established, especially by introducing new methods, ideas or products. In practise, this means that innovation happens at the frontier of the advancement of our society. It is the process that brought us from the hunter-gatherer society to the society we live in nowadays. Over the history of humankind, we worked to advance ourselves and improve our quality of living. For example, life expectancy increased from around 40 years in the 14th century up to around 80 years nowadays [1], [2], the global happiness increased significantly over the last three decades [3] and archeologic data shows that in the prehistoric times the level of violence was much higher than in the modern era [4]. Society has come a long way by innovation, but there is still a lot to improve: there are still people that are unhappy, die from disease and suffer from violence.

The noble thing of working on a PhD thesis is that one takes a few years the time to contribute to this advancement of humankind. The work of one person over the period of four years is in most cases too limited in scope to have a significant impact on the big topics mentioned earlier but it is a good opportunity to have a significant impact on a small field. And then eventually, a lot of small steps result in one big leap altogether.

1 Introduction

"From cardboard and duct tape to ABS polycarbonate, it took 5,127 prototypes and 15 years to get it right.

— James Dyson, 2011

The bearing is a machine component that has made significant progress compared to the early days: its lifetime has increased considerably, while at the same time friction has decreased significantly [5], [6]. Still, there is room for improvement as energy losses due to friction and system failures due to wear, cost society significant amounts of money and CO_2 emissions. Estimations shown in Figure 1-1 [7] show that in total about 23% (119EJ) of the world's total energy consumption is caused by tribological contacts, where approximately 20% (103EJ) is related to friction losses and about 3% (26EJ) is related to remanufacturing of worn and spare parts. From an economic perspective, the total cost of friction and wear add up to a total amount of 2 540 billion Euro globally. Figure 1-1 illustrates that of these costs, about 73% is related to friction and about 27% is related to wear.

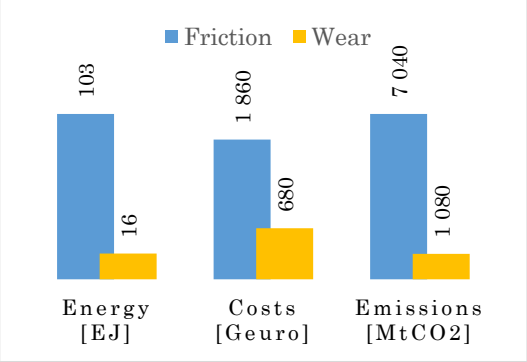

Figure 1-1 Losses due to tribological contacts [7].

The bearing and the dynamic contact seal (in this thesis regularly shortened to "seal") are two commonly used tribological components in engineering, since nearly all moving machines rely on them for proper operation. Their market values also illustrate this by being 102.2 billion Euro for bearings systems in 2018 [8] and 59.6 billion Euro for sealing (and gasket) systems in 2017 [9]. Even a small improvement in these components can have a big impact on both the economy and the environment. As with tribological contacts in general, the main problems in these systems are wear and friction [10]–[12]. Wear occurs when the two relatively moving surfaces touch and a small amount of material is lost or transferred. Friction is a result of energy dissipation when the two surfaces slide or roll with respect to each other. In addition to wear and friction, dynamic contact seals also suffer from the presence of leakage [13], [14] which is fundamental to both their function as well as their performance.

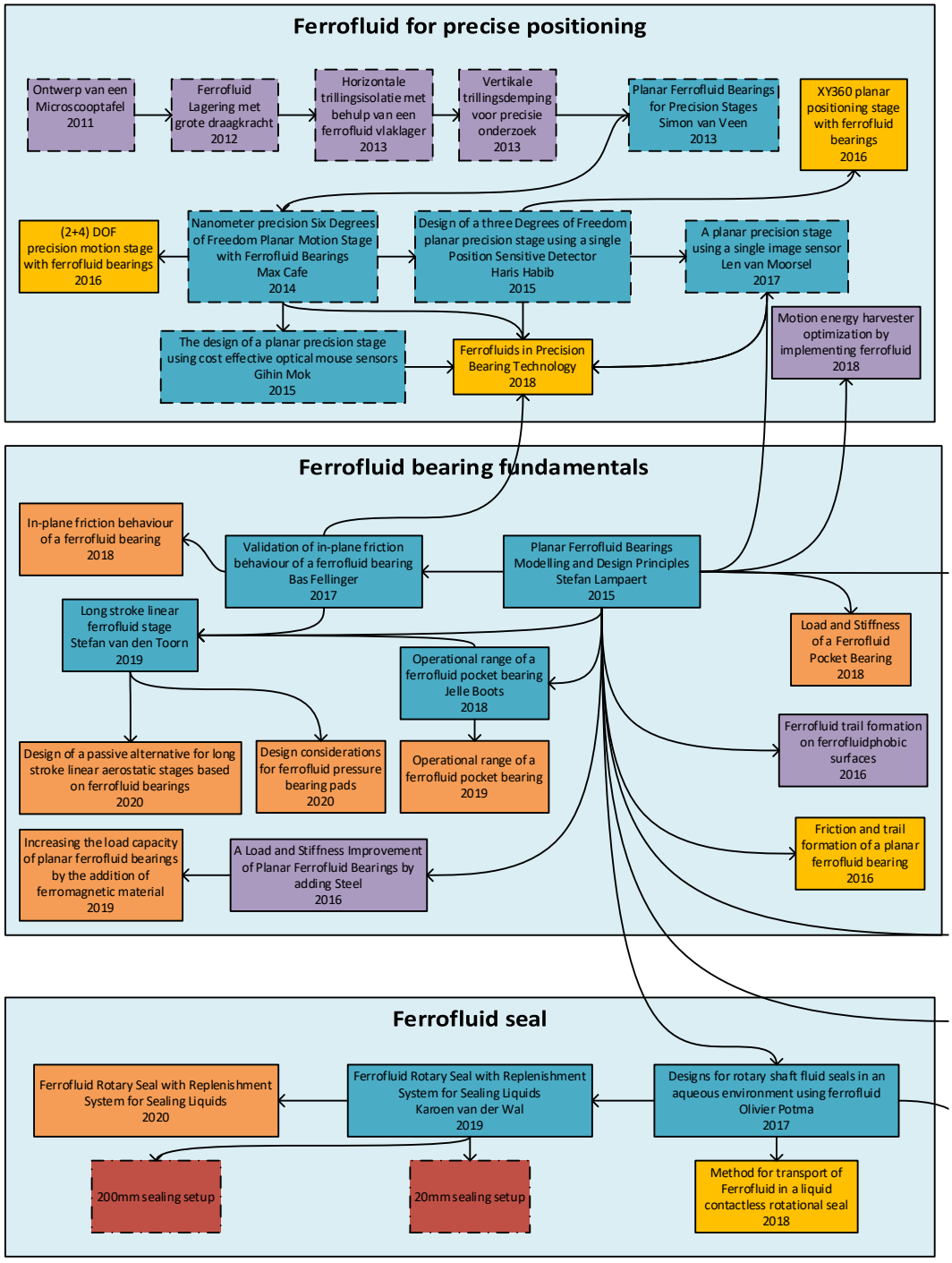
Ferrofluid for precise positioning
Ontwerp van een Microscooptafel 2011
Ferrofluid Lagering met grote draagkracht 2012
Horizontale trillingsisolatie met behulp van een ferrofluid vlaklager 2013
Vertikale trillingsdemping voor precisie onderzoek 2013
Planar Ferrofluid Bearings for Precision Stages Simon van Veen 2013
XY360 planar positioning stage with ferrofluid bearings 2016
(2+4) DOF precision motion stage with ferrofluid bearings 2016
Nanometer precision Six Degrees of Freedom Planar Motion Stage with Ferrofluid Bearings Max Cafe 2014
Design of a three Degrees of Freedom planar precision stage using a single Position Sensitive Detector Haris Habib 2015
A planar precision stage using a single image sensor Len van Moorsel 2017
Motion energy harvester optimization by implementing ferrofluid 2018
The design of a planar precision stage using cost effective optical mouse sensors Gihin Mok 2015
Ferrofluids in Precision Bearing Technology 2018
Ferrofluid bearing fundamentals
In-plane friction behaviour of a ferrofluid bearing 2018
Validation of in-plane friction behaviour of a ferrofluid bearing Bas Fellinger 2017
Planar Ferrofluid Bearings Modelling and Design Principles Stefan Lampaert 2015
Long stroke linear ferrofluid stage Stefan van den Toorn 2019
Load and Stiffness of a Ferrofluid Pocket Bearing 2018
Operational range of a ferrofluid pocket bearing Jelle Boots 2018
Ferrofluid trail formation on ferrofluidphobic surfaces 2016
Design of a passive alternative for long stroke linear aerostatic stages based on ferrofluid bearings 2020
Design considerations for ferrofluid pressure bearing pads 2020
Operational range of a ferrofluid pocket bearing 2019
Friction and trail formation of a planar ferrofluid bearing 2016
Increasing the load capacity of planar ferrofluid bearings by the addition of ferromagnetic material 2019
A Load and Stiffness Improvement of Planar Ferrofluid Bearings by adding Steel 2016
Ferrofluid seal
Ferrofluid Rotary Seal with Replenishment System for Sealing Liquids 2020
Ferrofluid Rotary Seal with Replenishment System for Sealing Liquids Karoen van der Wal 2019
Designs for rotary shaft fluid seals in an aqueous environment using ferrofluid Olivier Potma 2017
200mm sealing setup
20mm sealing setup
Method for transport of Ferrofluid in a liquid contactless rotational seal 2018

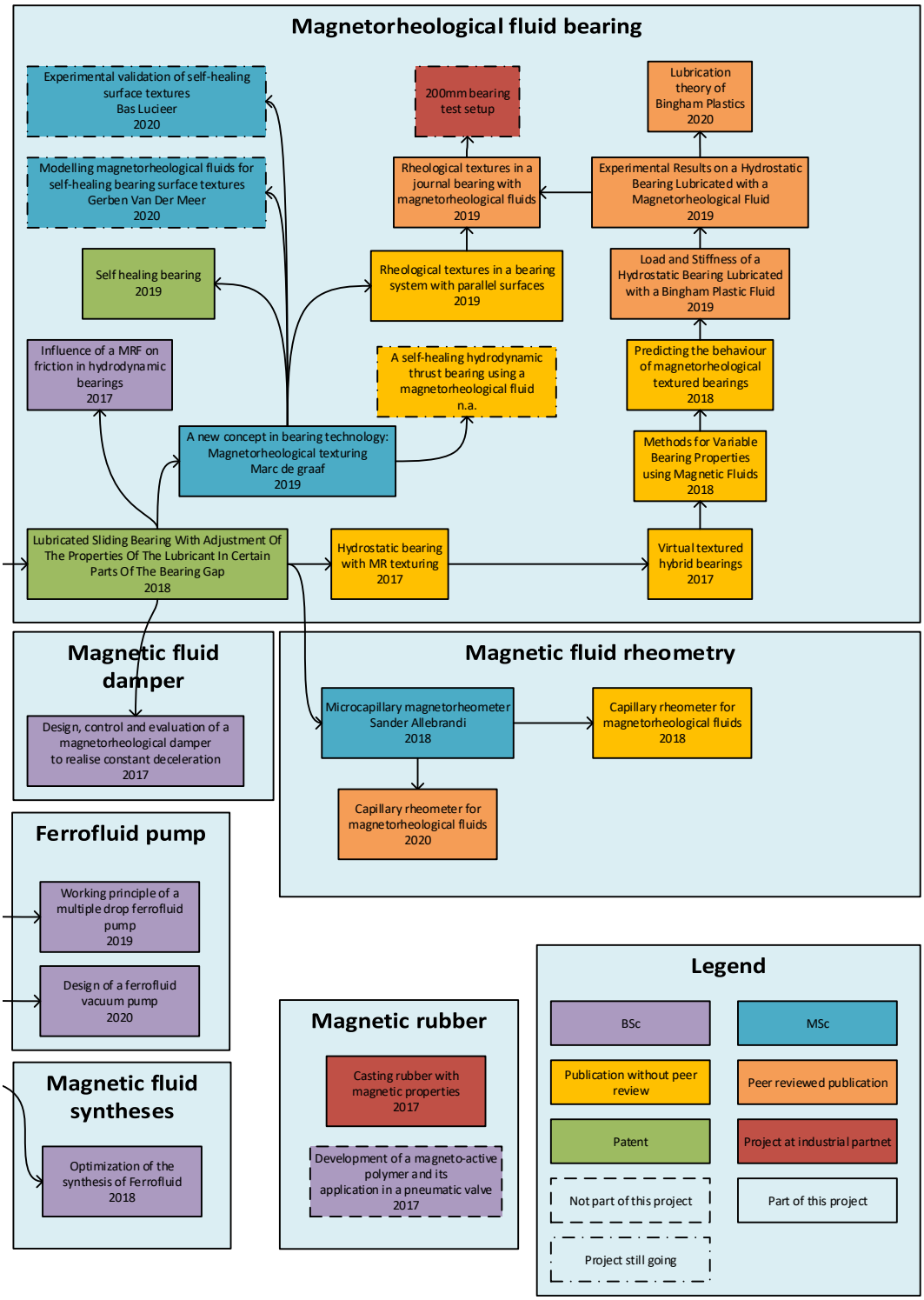

Figure 1-2: Graphical overview of the different projects, reports and publications from TU Delft related to the work of this thesis. All MSc reports are presented here with the name of the author, and all BSc reports have been written by student groups of 4. All other publications have been written by S. Lampaert, and all projects after 2015 have been supervised by S. Lampaert. See the appendices for a full reference of these publications and reports.

Even the correct working of a dynamic contact seal relies on a small lubricating film between the moving surfaces. As a result, dynamic contact seals always show some amount of leakage, without which the seal would suffer from excessive wear.

The question thus arises: how can we improve upon these systems? The application of magnetic fluids has proven to be beneficial for bearing [15]–[24] and sealing systems [25]–[33], but also in plenty of other applications like recycling [34]–[36], sensing [37]–[39], actuation [40]–[43], pumping [44]–[46], damping [47]–[49], cooling [45], [46], oil spill cleaning [50]–[52], wastewater treatment [53]–[55], medical MRI imaging [56]–[58], drug targeting [59]–[65] and cancer treatment [66]–[69]. Magnetic fluids consist of a suspension of magnetic particles in a carrier fluid. This gives them the unique properties of being attracted to a magnetic field and changing their rheological behaviour in reaction to a magnetic field. The attracting force is the result of the magnetic particles being attracted in the direction of the positive gradient of the magnetic field while taking the carrier liquid with them. The change in rheology is generally the effect of two phenomena that make the fluid effectively more viscous. The first is that the magnetic particles are unable to rotate in the magnetic field since they want to stay aligned with the magnetic field lines. The second is that the magnetic particles cluster together forming chains or other complex structures. These special properties of magnetic fluids can be used to give bearing and the sealing machine components unique behaviour that could potentially improve the performance.

The thesis has two main objectives. **The first objective is to further investigate the potential of magnetic fluids in bearing and sealing components.** This consists of exploratory, fundamental and early stage research. The unique properties of magnetic fluids are eventually used in ferrofluid bearings, ferrofluid seals, bearings with rheological textures and self-healing bearings. All of these concepts have resulted in fundamental new insights, resulting in various patents and publications in scientific journals.

The second objective is to develop the necessary knowledge to bring these concepts to society in the form of applications. This ended up in the development of different methods, models, and experimental setups each discussed extensively within this thesis.

In this thesis the term “magnetic fluids” is used as a general definition that includes both ferrofluids and magnetorheological fluids. Literature generally speaks of ferrofluid as a colloidal suspension of magnetic nanoparticles such that it is attracted by a magnetic field [70]–[75]. Magnetorheological fluids are generally defined by literature as suspensions of ferromagnetic micro particles such that they show a strong change in rheological behaviour in response to a magnetic field [75]–[79]. In practice, there is a large grey area between ferrofluids and magnetorheological fluids since colloidal suspensions exist which are both attracted to a magnetic field and strongly change rheology in response to a magnetic field [80], [81]. Therefore, this thesis chooses to use a slightly different definition. The work defines a fluid as a ferrofluid when the application predominantly uses the attracting force between the magnet and the fluids for achieving the desired performance. In contrast, this work talks about magnetorheological fluids when the change in rheological behaviour is predominantly used in the application. So, the application of the fluid defines the type of fluid, not what it is made of. In addition, most of the theory on magnetorheological fluids in this thesis is also applicable to electrorheological fluids.

Chapter 2 to 9 deal with the six different focus areas of this thesis: ferrofluid bearings, ferrofluid gas/fluid seals, rheological textures, lubrication theory for Bingham plastics, self-healing bearings and rheological characterization of magnetic fluids. Chapter 10 gathers all

the conclusions and chapter 11 gathers all recommendations of the different focus areas. The appendices contain all relevant publications made during this PhD research [82]–[96]. The main part of this thesis reuses some of the material of these appendices. Figure 1-3 displays the thesis structure in a graphical way. Figure 1-2 presents an overview of all the projects, reports and publications from Delft University of Technology related to this thesis.

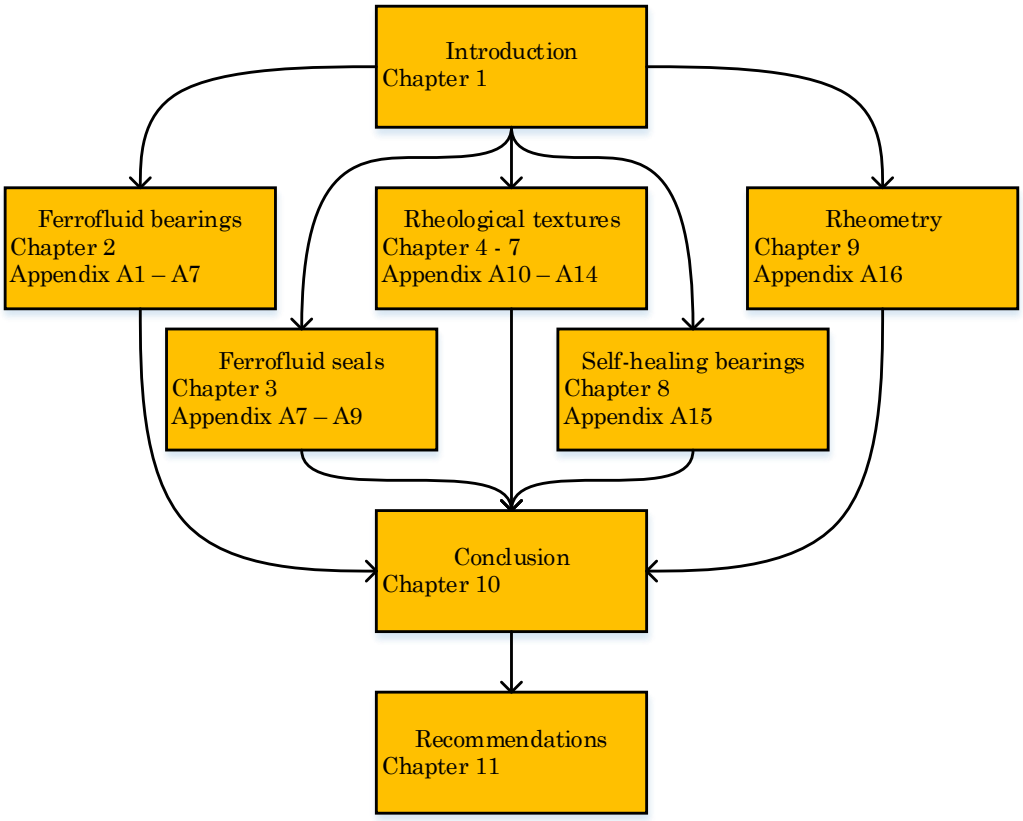

Figure 1-3: Thesis structure.

2 Ferrofluid bearings

"Leadership is not about being in charge. Leadership is about taking care of those in your charge"

— Simon Sinek, 2015

This chapter contains the highlights of the work presented in appendix A1 to A6. See these appendices for more background on the different topics discussed in this chapter.

Subjecting a ferrofluid to a magnetic field results in an internal pressure in the fluid that is capable of carrying a load [97]. This pressure is used to generate the load carrying capacity of a ferrofluid bearing, which as a result can be categorized as a type of hydrostatic bearing since it does not need a relative motion to maintain a lubricating film [98], [99]. The bearing distinguishes itself from other concepts by its low price, compactness, inherent stability, low (viscous) friction, absence of pumps and absence of stick-slip. This makes the bearing an interesting alternative to, for example, air bearings and magnetic bearings.

The maximum pressure developed within the fluid due to an external magnetic field typically can reach up to one bar, depending on the magnetic field strength and the type of ferrofluid [71]. In this thesis we distinguish two types of ferrofluid bearings. The first concept is the ferrofluid pressure bearing (Figure 2-1) that directly uses the induced pressure to create a load carrying capacity [97]. The second concept is the ferrofluid pocket bearing that indirectly uses the induced pressure to create a load carrying capacity [98], [99]. The induced pressure creates a ferrofluid seal that encapsulates a pocket of air that carries the load (Figure 2-2). Both of these bearing concepts are discussed extensively in the next section and in appendix A1.

These two bearing concepts already have received attention in literature prior to this research, but the knowledge was lacking on how to design such a bearing concept according to desired specifications [15]–[24]. The lack of this knowledge made it very troublesome to implement it in industry.

Therefore, the goal of the work on ferrofluid bearings in this project was to generate the necessary knowledge and design rules to predict the behaviour of ferrofluid bearings. This knowledge included models and methods to predict different bearing properties like load capacity, stiffness and friction as a function of design parameters like geometry, shape of the magnetic field and properties of the ferrofluid. The final result of this research line is a ferrofluid bearing setup that demonstrates that this goal was achieved in the end.

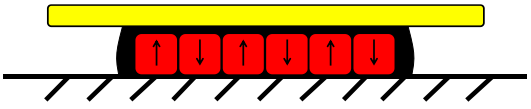

Figure 2-1: Example of a ferrofluid pressure bearing.

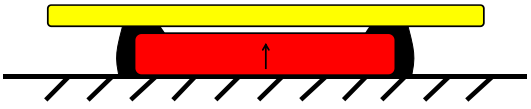

Figure 2-2: Example of a ferrofluid pocket bearing.

2.1 Load capacity & stiffness

A ferrofluid subjected to a magnetic field develops a magnetic body force that creates a pressure inside the fluid [70]. This effect is comparable to the gravity force on a body of fluid; at the upper surface of the fluid there is only ambient pressure, but at the bottom of the fluid there can be a very high pressure resulting from the gravity acting on the water column sitting on this location. The ferrofluid is distributed in a similar way across the magnet as the water in the oceans is distributed across earth. The load capacity of a ferrofluid pressure bearing is the result of this internal pressure created by the magnetic body force. One may say that the bearing is floating on top of a volume of ferrofluid. The total force developed by this effect increases closer to the magnet since the body force is larger there due to the distribution of the magnetic field around the magnet. This change in pressure and thus load capacity as a function of the displacement defines the stiffness of the bearing.

The ferrofluid pocket bearing works slightly different compared to the pressure bearing. In this case a ferrofluid seal encapsulates and pressurizes a volume of non-magnetic fluid such that the pressure in the non-magnetic fluid predominantly carries the load. Figure 2-3 shows an example of such a bearing in which a ring magnet captures a certain volume of ferrofluid that in turn encapsulates a pocket of air. In this bearing system, the pressure that the ferrofluid seal is able to withstand predominantly defines the load capacity. Appendix A1 presents more information on the modelling of these types of bearings.

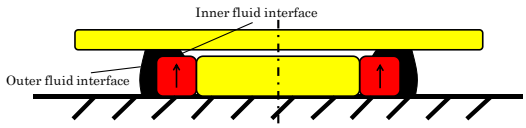

Figure 2-3: Ferrofluid pocket bearing using a ring magnet.

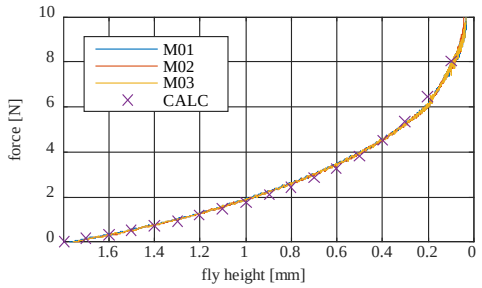

Figure 2-4: Load capacity as a function of the fly height for a pocket bearing.

Figure 2-4 presents both the modelled and measured maximum load capacity as a function of the fly height corresponding to the pocket bearing configuration of Figure 2-3. The point of maximum load capacity is defined by the situation where air starts to leak through the seal. This line of maximum load capacity is of interest since it defines the load that the bearing configuration can maximally handle for that specific fly height. The graph shows a close fit between the measured data and the analytical model, showing that the model accurately describes the maximum load capacity. The operational range of this bearing is covered later in this chapter.

One way to increase the normalized bearing pressure is to use multiple sequential sealing stages in the bearing. Figure 2-5 shows such a bearing configuration to increase the normalized load capacity. In addition, this configuration uses two ferromagnetic rings so that the magnetic field at the seals increases, resulting in a higher load capacity. Figure 2-6 presents the corresponding load capacities as a function of the fly height for both the model and the measurements. The graph also shows the difference in the system with and without the ferromagnetic rings. Again, the data shows a good fit between the measurements and the predictions. Appendix A4 presents more information on the modelling of this type of bearing.

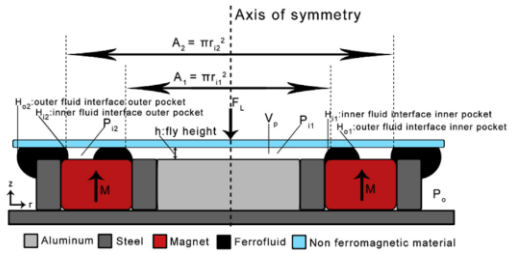

Figure 2-5: Ferrofluid pocket bearing using two sequential seals to increase stiffness and load capacity. (see appendix A4 for symbols)

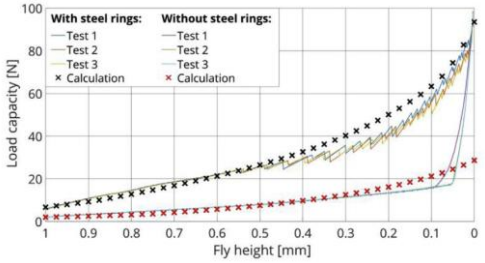

Figure 2-6: Load capacity as a function of the fly height of a ferrofluid pocket bearing using two seals, with and without steel rings.

The two previous models do not accurately include the in-plane translation of the seal when the bearing faces move towards each other. The resulting error in these models is only minor for these designs, but it might become significant for other designs. Therefore, the goal was to develop a tracking model for the position of the ferrofluid seal. The challenge was to properly track the mass conservation of the ferrofluid such that the correct ferrofluid interfaces were picked. Appendix A5 presents more information on the modelling method. Figure 2-8 presents the results of this method along with the corresponding experimental validation. Figure 2-7 presents the bearing design on which the results are based. The graph demonstrates that the bearing can both push and pull; the system is able to cope with positive and negative normal forces. Figure 2-9 shows the normalized maximum and minimum load carrying capacity of this bearing. The lines of maximum and minimum load capacity enclose an area that defines the stable operation region; the system does not leak any air through the seal in this region.

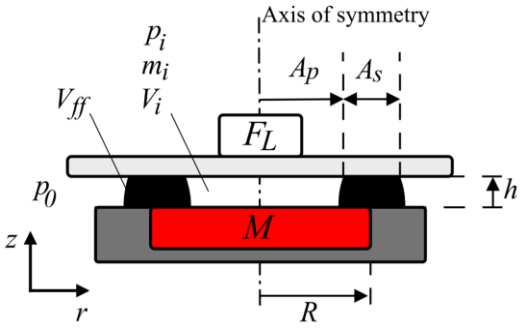

Figure 2-7: Ferrofluid pocket bearing using a disc magnet. (see appendix A5 for symbols)

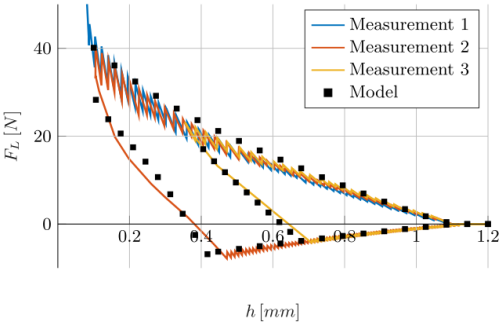

Figure 2-8: Load capacity as a function of the fly height of a ferrofluid pocket bearing.

The normalized load capacity of a ferrofluid pocket bearing is predominantly defined by the sealing capacity of the ferrofluid seal, and in a similar way the normalized stiffness of a ferrofluid pocket bearing is predominantly defined by the stiffness of the seal. The stiffness of the bearing can be derived from the stable operational range presented in Figure 2-9 since this is the gradient of the curve in the stable region.

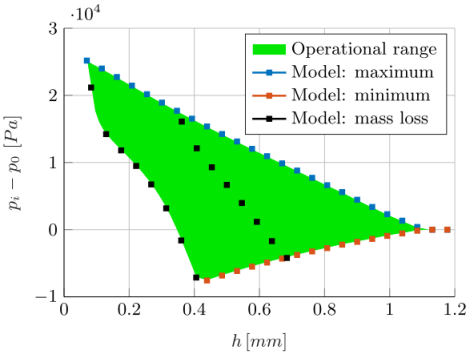

Figure 2-9: Operational range of a ferrofluid pocket bearing.

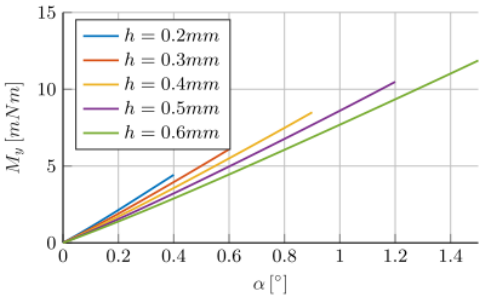

Figure 2-10: Tilting moment capacity as a function of the tilting angle for a ferrofluid pocket bearing.

The tilting moment capacity is also important for the design of a ferrofluid bearing. Inspired by the method used for Figure 2-9 a new method is derived that considers the tilting of the bearing. Figure 2-10 presents the results of this model for the bearing configuration presented in Figure 2-7.

2.2 Friction

The ferrofluid bearing always has a lubricating film between the bearing surfaces during normal operation. This absence of mechanical contact guarantees that the surfaces do not wear. It also guarantees that the bearing exhibits viscous friction and complete absence of stick-slip. This is especially interesting for positioning systems since the result of this is a well-defined linear behaviour. Knowing the friction of a bearing in a system during the design phase is of utter importance since, for example, this defines the part of the force needed for motion and the related heat dissipation in the bearing and the actuator.

When the ferrofluid bearings presented in the earlier section is slide to the counter surface, the major part of the fluid stays near the magnets. Modelling the friction with the use of a pure Couette flow model would therefore be incorrect since this would predict a net fluid transport (see appendix A2). Based on the assumption that there may not be any fluid transport under in the bearing, a new friction model has been derived that assumes the flow profile given in Figure 2-11. This fluid profile consists of a summation of a Couette flow and a Poiseuille flow in such a way that there is no net fluid transport present. These assumptions are correct since we are considering a low Reynolds number flow.

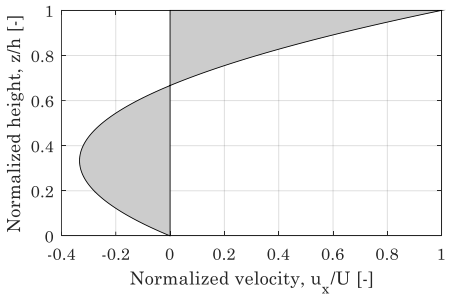

Figure 2-11: Flow profile that shows no net fluid transport. This profile is assumed for the friction of a ferrofluid bearing.

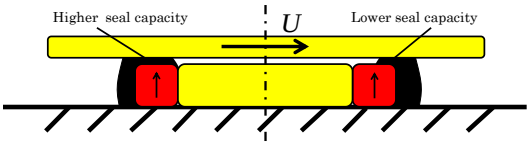

Figure 2-12: Ferrofluid pocket bearing under translation.

The sliding motion between the two surfaces results in a Couette flow and the gradient in the magnetic field results in a Poiseuille flow. The gradient in the magnetic field also needs to provide the sealing capacity, meaning that the magnetic field has to deliver an additional force during translation. When the magnetic field is not strong enough to deliver this force, the seal breaks and air leaks out of the pocket (Figure 2-12). This leads to the observation that the maximum load capacity of a ferrofluid pocket bearing reduces as a result of the sliding velocity.

Figure 2-13 presents an experimental validation of this model by presenting the compliance plot in the frequency domain of the setup presented in Figure 2-15. This plot presents the damping coefficient as it effects the quality factor of the resonance frequency. The stiffness in this system is a pure control stiffness since the system has no lateral stiffness from itself. The dash-dot line in the graph presents the damping line that would be expected from the model. The graph shows that the experimental results are close to the model, thereby demonstrating the validity of the model. Appendix A2 present a more extensive analysis on the friction of a ferrofluid pocket bearing.

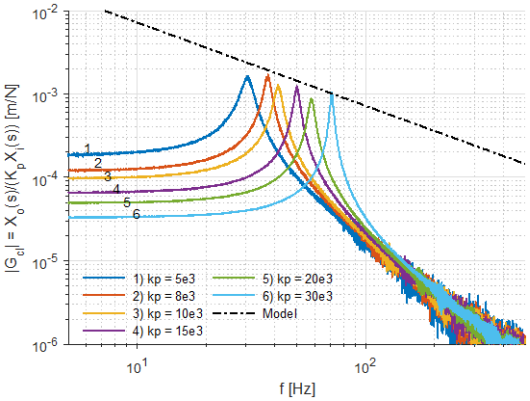

Figure 2-13: Transmissibility plot of a positioning system using ferrofluid bearings.

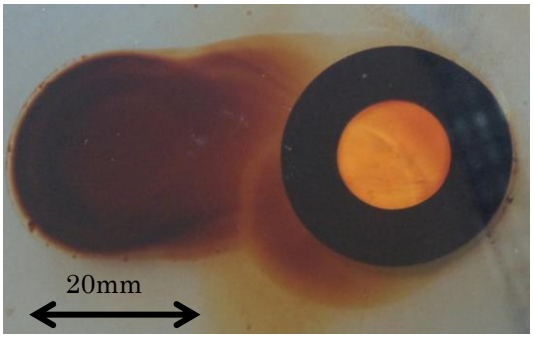

Figure 2-14: Picture of a typical trail formation of a ferrofluid bearing.

A challenge with these types of bearings is the repeatability in flight height. Translating the bearing in plane leaves a trail of ferrofluid that causes less fluid to be available for carrying a load. In the case of a pocket bearing this can cause air to escape from the seal; the reduced amount of ferrofluid causes a reduced sealing strength. The loss of air results in a permanent change in fly height. This phenomenon should be considered during the design of a ferrofluid bearing such that it does not negatively influence the performance.

2.3 Ferrofluids for precise positioning

The previous sections demonstrate the current understanding of the ferrofluid bearing and the logical next step is to use this knowledge for an application. One of the demonstrators realized before the start of this project is presented in in Figure 2-15 and Figure 2-16. This system was redesigned using the knowledge gained in this project to improve the control of the mover. The system functions as a positioning system that is able to move in 6 degrees of freedom. The focus of this system was to prove that ferrofluid pocket bearings, having no stick slip, enable nm precision positioning with high control bandwidth. The application in mind was fast scanning microscopy and 3D nano-printing. The novelty in the design of this system is in the dual use of the magnets as ferrofluid bearings and field generators for Lorentz actuation. The result is an integrated bearing-actuator system. Appendix A2 and A3 present a more extensive discussion on ferrofluid bearings in precise positioning.

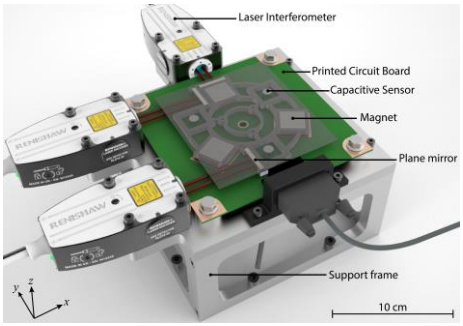

Figure 2-15: Positioning system with six degrees of freedom build prior to this project but redesigned for the work on the friction of ferrofluid bearings.

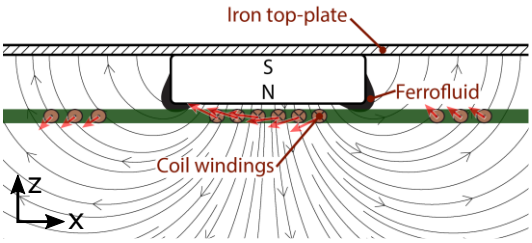

Figure 2-16: The magnets used for actuation are also used for the ferrofluid bearings, thereby integrating the actuator and bearing system.

During this PhD project a lot of fundamental theory of ferrofluid bearings was developed [82], [83], [91], [92]. To bring the ferrofluid bearing to a point where it is mature enough to be further developed by industry a new target was selected: To design and build a ferrofluid long stroke stage that closely resembles an industrial precise positioning air bearing system. The result was the system of Figure 2-17 that has a load capacity of about 120N, a stiffness of about 0.5 N/µm and a damping coefficient of about 3 Ns/m. Figure 2-18 shows that the system has a good repeatability by showing the change in fly height as a function of the speed at which the mover translated back and forth. The performance of the system in general shows that the concept is able to meet specifications that are desired by industry. This shows that the ferrofluid bearing is at a point where it is mature enough to be further developed by industry. The concept is now technically validated and is waiting for a market validation. Appendix A6 presents the complete analyses on this latest ferrofluid bearing.

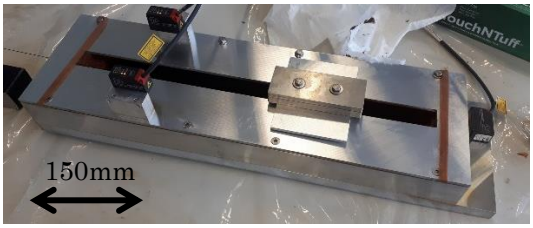

Figure 2-17: Picture of the ferrofluid long stroke stage.

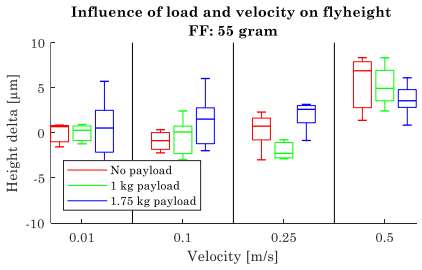

Figure 2-18: Repeatability in fly height as a function of the translational velocity. The colours present different loading conditions.

3 Ferrofluid gas/liquid seals

"Only those who dare to fail greatly can ever achieve greatly."

— Robert F. Kennedy, 1966

This chapter contains the highlights of the work presented in appendix A8 and A9. See these appendices for more background on the different topics discussed in this chapter.

The invention of the ferrofluid seal dates back to the patent of 1971 by Ronald Rosensweig as co-founder of the company Ferrofluidics Corporation, now part of the Ferrotec Corporation [100]. The seal works in a very similar way as the pocket bearing discussed in Chapter 2: a local magnetic field captures a volume of ferrofluid such that it creates a barrier between two volumes, as shown in Figure 3-1 [101]. The seal distinguishes itself from other dynamic sealing systems by being insensitive to wear [14], [102], while achieving much lower leakage rates [13], [14]. It is therefore a proven product to seal gasses and vacuums for already multiple decades [25]–[33]. However, the seal has not yet proven itself to be a good liquid seal up to now. Literature shows that the seal eventually fails over time when sealing liquids, the exact reason is currently not properly understood [103]–[124].

There exist two hypotheses why the seal eventually fails over time. The first hypothesis is that the ferrofluid degrades over time due to some chemical reaction. This lowers the saturation magnetization over time resulting in a lower sealing capacity that eventually causes sealing failure [121]. The second hypothesis is that the ferrofluid is washed away over time resulting in decreasingly less ferrofluid in the seal [104]. This also causes the sealing capacity to lower, eventually causing sealing failure.

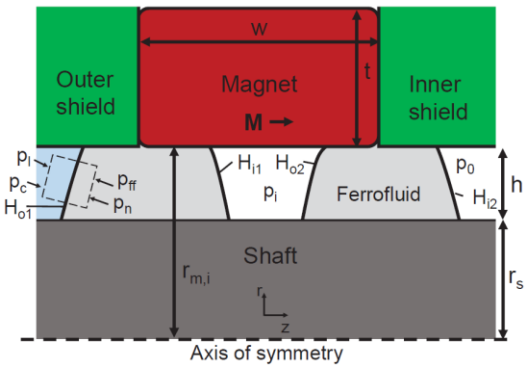

Figure 3-1: Two seals formed in a thin slit by local magnetic fields.

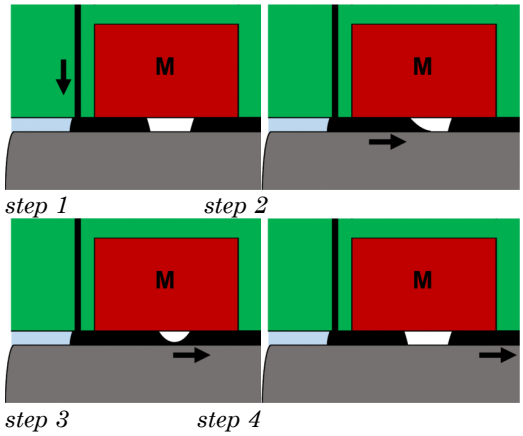

Figure 3-2: Picture of the flow during replenishing.

3.1 Replenishing system

To solve this, the idea was developed to replenish the ferrofluid during operation. Whatever the root cause (ferrofluid removal or ferrofluid degradation), constantly adding new ferrofluid to the system theoretically solves the problem. This idea seems trivial but it is not since the ferrofluid must be able to flow between the different sealing steps in a multi stage seal without simultaneously leaking the medium that it tries to seal. Figure 3-2 illustrates the process of replenishing the ferrofluid. Step 1 contains the normal condition of the ferrofluid seal. At step 2, some ferrofluid enters the first seal by an external supply. When the volume of the ferrofluid exceeds a threshold value, some volume leaks to the second seal as shown at step 3. This happens without any leakage of the fluid that is being sealed. Then the system goes to step 4 where the system is back at rest and where fresh ferrofluid is at the first seal.

The replenishment of the ferrofluid creates a sealing system where the conditions are kept close to the initial conditions. This practically means that when the system is able to work at the initial stage, the system keeps on working from that time on. Appendix A8 and A9 contain more detailed information on this sealing technology.

3.2 Experimental validation

The experimental validation of the replenishing idea has been realized in two different experimental setups, Figure 3-3 and Figure 3-4 show the first setup and Figure 3-5 shows the second setup. Both setups contain a rotating shaft with a radial clearance (= sealing gap) of 0.1mm that enters a pressure chamber with water. The first setup uses three magnets and a nonmagnetic shaft such that a critical pressure of 34 kPa was achieved. The second setup uses one magnet and a magnetic shaft such that a critical pressure of 76 kPa was achieved. A syringe pump supplies the ferrofluid to the first seal with a constant rate such that it can flow through the different sealing steps. The excessive ferrofluid flows out of the system at the last seal and is discharged.

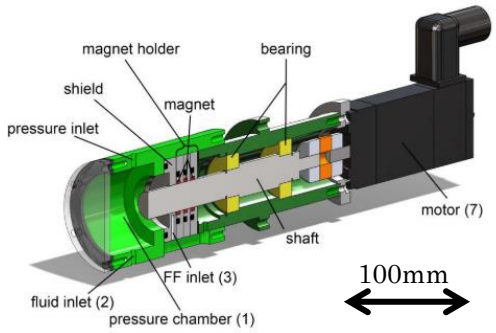

Figure 3-3: Drawing of the first experimental setup to test the ferrofluid seal with replenishing system.

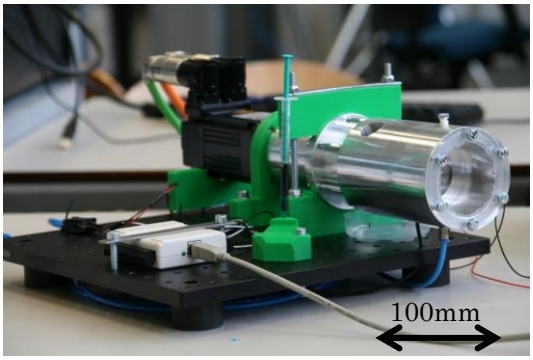

Figure 3-4: Picture of the first experimental setup to test the ferrofluid seal with replenishing system.

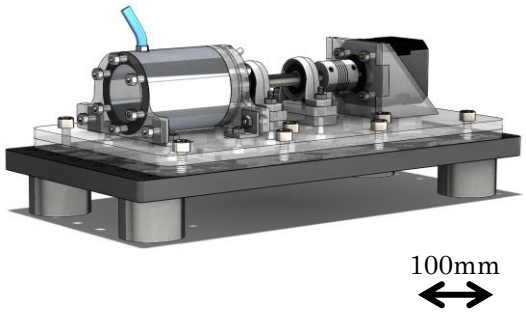

Figure 3-5: Drawing of the second experimental setup to test the ferrofluid seal with replenishing system and 10mm shaft diameter

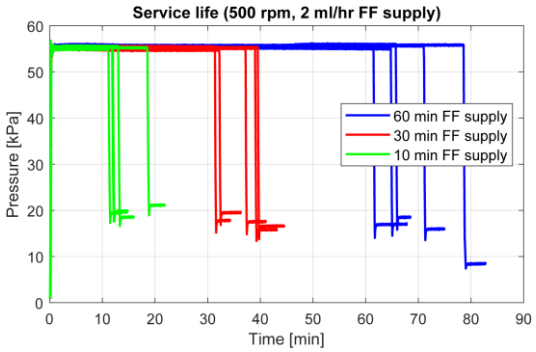

Figure 3-6: Pressure over time for a ferrofluid seal with replenishing system. The different colours present different terminations times of the replenishing system.

Both systems showed an increase in sealing lifetime as a result of the replenishing of the ferrofluid. Figure 3-6 shows the sealing pressure over a certain time period of the second setup showed in Figure 3-5. The sealing pressure here was selected to be close to the critical sealing pressure to ensure that the seal fails quickly (within minutes). The graph shows an experiment where the replenishing system shuts off after 10 minutes for the green lines, 30 minutes for the red lines and 60 minutes for the blue lines. For every set of measurements, it is visible that the system fails shortly after deactivation of the replenishing system. This is in good accordance with results from literature that also show quick system failure when working close to the critical pressure.

These results demonstrate that as long as the replenishing system keeps working, the ferrofluid seal keeps working. With this solution, the problem of sealing failure over time is solved and a seal is realized that has complete absence of leakage, low friction and 'infinite' lifetime. To further develop this technology, a third test was built with a 20mm shaft by the industrial partner in these projects. The setup showed similar results compared to the second setup in Figure 3-5, increasing the confidence in the repeatability of the results in other systems. Currently a fourth sealing setup with a 200mm shaft is in production at the industrial partner. This setup has as primary goal to validate that a scaled-up version of the concept still functions properly.

4 Basics of rheological textures

The critical ingredient is getting off your butt and doing something. It's as simple as that. A lot of people have ideas, but there are few who decide to do something about them now. Not tomorrow. Not next week. But today. The true entrepreneur is a doer, not a dreamer.

— Nolan K. Bushnell, 2004

This chapter discusses the fundamental concepts used in chapter 5 and 6. See those chapter for more information on the applicability of the theory.

When one designs a bearing, generally, one mainly designs the geometry of the bearing faces [11], [125]. The separation between the bearing surfaces varies from one point to the other, resulting in a non-uniform height distribution of the lubricating film. This non-uniform distribution causes a certain pressure distribution and friction force, defining the characteristics of the bearing. An example is a journal bearing that has a converging wedge and a diverging wedge that causes respectively a high pressure region and a low pressure or even cavitation region. Another example is a hydrostatic bearing that uses a recess area where the pressure will be uniform and a land area with a pressure drop from the edge of the recess to the edge of the bearing. Fundamentally, two phenomena occur when the spacing between the bearing surfaces are reduced: The flow resistance of the lubricant increases and the lubricant transportation rate decreases (due to the relative motion between the bearing surfaces, see Figure 4-1 and Table 4-1). So, normally when you design a bearing you design a film height geometry, but what you are actually doing, is that you are designing for a desired local flow resistance and lubricant transportation rate.

Table 4-1: Indication of the effect of the different textures on the flow resistance and lubricant transportation rate.

	Geometrical texture	Rheological texture with constant field	Rheological texture with gradient field
Flow resistance	↑	↑	↑
Lubricant transportation rate	↓	0	↑/↓

Starting from this point of view, one can also think of other methods to achieve a variation of lubricant flow resistance and lubricant transportation rate. The three methods that can be varied to change the system performance are the geometry of the channel, the rheological behaviour of the fluid and the interface between the lubricant and bearing surface. The work in this chapter focuses predominantly on the potential of a change in the rheological behaviour of the lubrication fluid to achieve a desired behaviour, further referred to as "rheological textures". The work in this thesis considers three different choices to change the rheological behaviour: magnetorheological fluids with a magnetic field [126]–[130], electrorheological fluids [131], [132] with an electric field and conventional lubricants with a change in temperature [125]. The theory of this chapter is explained in the context of magnetorheological fluids and a local magnetic field, but is also equally applicable to electrorheological fluids and local electric fields [133]. The scientific literature already contains an extensive discussion on the applications of smart fluids (magnetorheological and electrorheological fluids [79], [133]) in bearing systems, but most of the literature focusses on changing the rheology of the lubricant in the bearing system as a whole, not just locally [134]–[150].

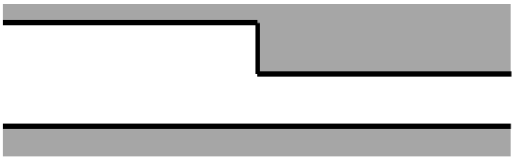

Figure 4-1: The Rayleigh step bearing, a geometrical texture.

In Newtonian lubrication theory, the shape of the fluid flow in the lubrication film fundamentally consists of a summation of a Poiseuille flow and a Couette flow. The Poiseuille flow is the result of the pressure gradient and is therefore directly related to the lubricant flow resistance. The Couette flow is the result of a relative movement between the bearing surfaces and is therefore directly related to the lubricant transportation rate. With a rheological texture, this is similar but not necessarily the same (see Figure 4-1, Figure 4-2 and Table 4-1).

Assume a lubrication configuration as presented in Figure 4-2 where the pressure p_1 is unequal to the pressure p_2, where the walls are static, where the magnetic field is constant over the height and where the lubricant is a magnetorheological fluid. Figure 4-2 demonstrates that the rheological texture causes a small reduction in pressure at the non-activated region and a large reduction in pressure at the activated region. At the activated region, the effective viscosity of the fluids is increased resulting in a higher flow resistance. It is evident here that the magnetic field in combination with a magneto-rheological fluid creates an increased flow resistance in the bearing gap without the use of a reduced film height, a so-called rheological texture.

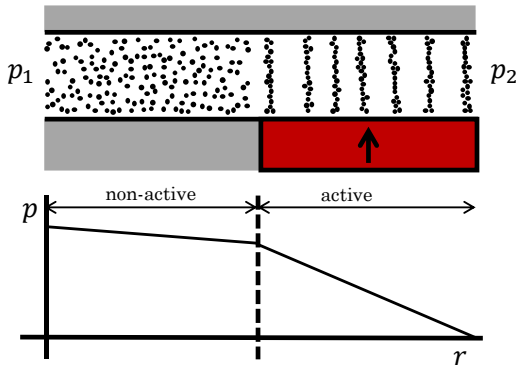

Figure 4-2: Rheological texture with a constant magnetic field. The pressure distribution assumes a differential pressure and static walls.

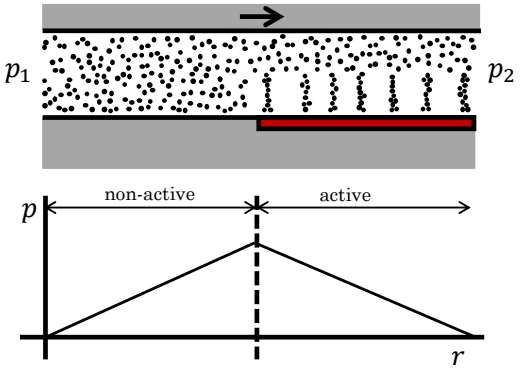

Figure 4-3: Rheological texture with a declining magnetic field. The pressure distribution assumes a translating surface.

Now assume the lubrication configuration of Figure 4-2 where the pressure p_1 is equal to the pressure p_2 and where the walls are sliding relative to each other. The fluid transport due to this sliding movement does not result in any change in pressure, in contrast to the case with a geometrical texture where a change in pressure would occur. The fluid transport in the non-active region is identical to the fluid transport in the active region due to uniform rheological properties across the height of the channel. The active region does have a higher shear stress with respect to the non-active region due to the increase in effective viscosity. The example demonstrates that this rheological texture does change the local flow resistance but does not change the lubricant transportation rate.

To be able to achieve a pressure gradient with a rheological texture as a result of a sliding movement between the bearing surfaces, one can use the lubrication configuration presented in Figure 4-3. In this configuration the pressure p_1 is equal to the pressure p_2, the walls are translating with respect to each other and the lubricant is a magnetorheological fluid, however in this case the magnetic field is reducing over the height. The reduction in magnetic field across the height of the lubricating film causes a reduction in effective viscosity across the height of the film. This results in a change in lubricant transportation rate that changes the pressure along the channel as shown in Figure 4-3. Note that this rheological texture also still has a flow resistance as is the case for the rheological textures using constant rheological properties across the channel.

In the situations mentioned in this chapter, it is evident that the conventional Newtonian iso-viscous lubrication theory does not hold anymore. The fundamental assumption that the flow consists of a certain summation of a Poiseuille flow and a Couette flow is not valid anymore. In this research, there was the need for a computationally efficient method to predict the bearing properties of certain bearing designs with rheological textures. This resulted in the development of a new lubrication theory for Bingham plastics discussed in chapter 7 and in appendix A14. This new theory has been derived for the situation where the rheological properties are constant across the height of the lubricating film. At this moment, modelling the bearing behaviour where the rheological properties of the lubricant vary across the height of the film, still has to be done with the use of a full CFD simulation and the Bingham-Papanastasiou material model. There might be more computationally efficient methods to do this, like adapting the method developed in appendix A14, but this was ultimately not the focus of the research presented in this thesis and is a topic of current research.

The concept of rheological textures challenges the idea that the performance of a bearing can only be optimal for one certain bearing speed together with one certain loading condition. By using external activation of the rheological textures, optimal performance is achievable for a complete range of speeds together with a complete range of loading conditions. Using magnetic fluids in combination with an active field creates the possibility of adding active control to the bearing to increase bearing properties like stiffness, damping and film height, something already discussed extensively in literature [17], [133], [143], [147], [148], [151]–[159].

Based on the philosophy of designing for flow resistance variations and lubricant transportation rate variations, the project patented a multitude of new bearing designs, demonstrating the novelty of rheological textures [87].

5 Rheological textures in thrust bearings

"When it comes to taking risks, I believe there are two kinds of people: those who don't dare try new things, and those who don't dare miss them."

— John C. Maxwell, Failing Forward: How to Make the Most of Your Mistakes

This chapter contains the highlights of the work presented in appendix A9 to A12 and [87]. See these sources for more background on the different topics discussed in this chapter.

This chapter discusses the applications of rheological textures in two different thrust bearing designs. The first design is a hydrostatic bearing that uses rheological textures with a constant magnetic field across the film. The second design is a hydrodynamic thrust bearing that uses a gradient magnetic field across the height of the film.

5.1 Hydrostatic bearing

To be able to demonstrate that a rheological texture behaves similarly to a physical texture, a theoretical model is derived to predict the performance which is then validated by some basic experiments. The rheological textures use a constant magnetic field across the film here (see chapter 4). The work roughly continues on the prior work of [17], [146], [158], [160]. Figure 5-1 presents the geometry assumed for the theoretical model. With this embodiment, it was easy to create a simple and controlled environment to develop the first insights early in the project. Figure 5-2 presents both the analytical model and the numerical model that describe the load capacity of this bearing configuration as a function of its channel height. The graph demonstrates that the analytical and numerical method have a good correspondence, providing a validation of both theory and the numerical model. Interesting to note from this graph is that the yield stress of the lubricant causes the -1 slope in the curve. A -3 slope would be expected from a geometrical texture, thereby demonstrating that rheological textures are similar to but not exactly the same as geometrical textures. See appendix A9 for more information on the theoretical and numerical model.

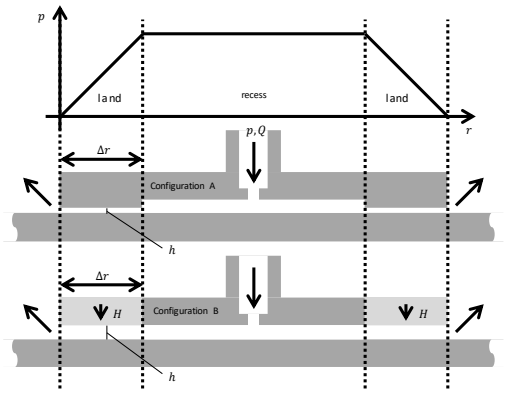

Figure 5-1: A hydrostatic bearing with geometrical textures (A) and rheological textures (B). The graph at the top presents the resulting pressure profile. (see appendix A9 for symbols)

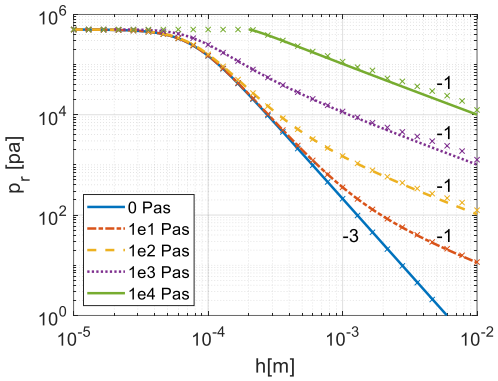

Figure 5-2: Specific load capacity as a function of the fly height for configuration B.

The main part of the experimental setup for the hydrostatic bearing consists of two circular bearing surfaces facing each other. Figure 5-3 presents a drawing of the main components and Figure 5-4 presents a picture of the same setup. The setup is basically the same as the system from Figure 5-1. An electromagnet enables the control of the magnetic field magnitude in the bearing gap. An external actuator system is used to press the surfaces on top of each other. A load sensor and displacement sensors take care of measuring the load as a function of the fluid film height. See appendix A11 for more information on this experimental setup.

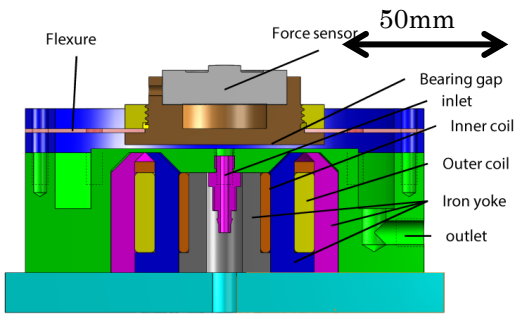

Figure 5-3: Drawing of the experimental setup to test the hydrostatic bearing with rheological textures, related to Figure 5-1 B.

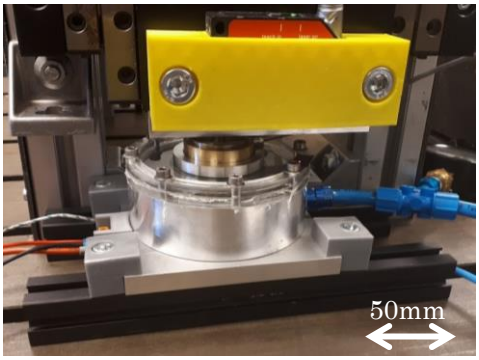

Figure 5-4: Picture of the experimental setup to test the hydrostatic bearing with rheological textures.

The analytical model, numerical model and experimental setup are generally in close agreement but there are some notable differences. Figure 5-5 shows that all three methods are in close agreement at large film heights but show some larger differences at low film heights. The experimental setup gives slightly lower results in bearing load than the other two methods, most probably due to some inaccuracies in the experimental setup. Nevertheless the trend in the results is very similar.

The difference between the analytical model and the numerical model in this situation can be explained using Figure 5-6 that presents the pressure distribution in the fluid film. The analytical model assumes a constant pressure in the recess part of the bearing and a

linear drop in the land area of the bearing. The numerical model shows that this is just a rather coarse estimation since the pressure already starts to drop in the recess area and the pressure continues to go down following an s-shape in the land area of the bearing. Appendix A11 contains a more extensive discussion on the experimental results of hydrostatic bearings.

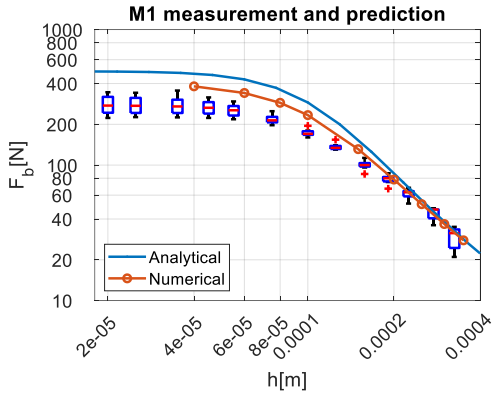

Figure 5-5: Load capacity as a function of the fly height for the measurements, analytical model and numerical model.

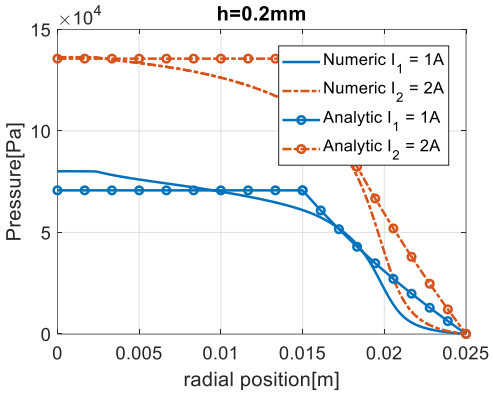

Figure 5-6: Pressure as a function of the radial position. Both the results from the numerical model and the analytical model is present.

5.2 Hydrodynamic bearing

This section discusses the effect of rheological textures using a gradient field in a hydrodynamic thrust bearing. The goal here was to model the performance of a hydrodynamic bearing using rheological textures that have varying rheological properties across the height of the lubricating film.

Chapter 4 shows that to realize a pressure field with rheological textures in a hydrodynamic bearing, it is key to create a variation in rheological properties across the height of the lubricating film. This is possible, for example, by the use of a reducing magnetic field across the film height in combination with a magnetorheological fluid. One way to realize this field shape is to use relatively small magnets together with a ferromagnetic material that surrounds them at one side of the bearing surface and a plain nonmagnetic surface at the other side of the bearing. Figure 5-7 shows such a configuration with the corresponding magnetic field.

This gradient in the magnetic field causes the magnetorheological fluid to be relatively viscous at the bottom surface and relatively thin at the upper bearing surface. Figure 5-8 and Figure 5-9 show the velocity profile achieved with this configuration. The results are generated using a CFD method that uses the Bingham-Papanastasiou material model [161] to approximate the yield stress behaviour. The yield stress of the fluid is a function of the magnetic field that is calculated in the same model. The figure shows a relative low flow speed at the bottom bearing surface and a relatively high flow speed at the upper bearing surface. Note that the shape of the flow is different from that of a normal Couette flow.

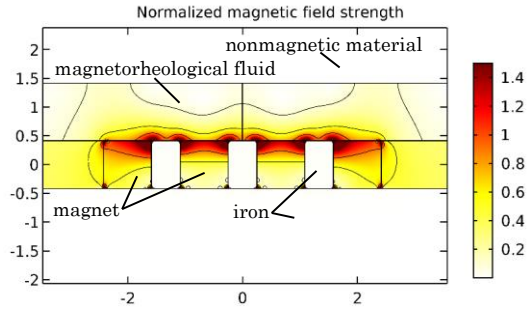

Figure 5-7: Magnet configuration to achieve a high field at one side and a weak field at the other side.

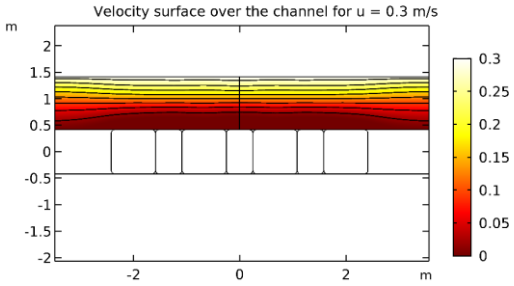

Figure 5-8: Flow field of a rheological texture that uses a gradient in the magnetic field.

This variation in the flow profile corresponds with a variation in the pressure along the film presented in Figure 5-10. The figure shows similar behaviour as present in a conventional Raleigh step bearing lubricated with a Newtonian fluid. This demonstrates that it is possible to achieve a load carrying capacity with two parallel surfaces with the use of rheological textures only. Appendix A12 contains more information on this concept.

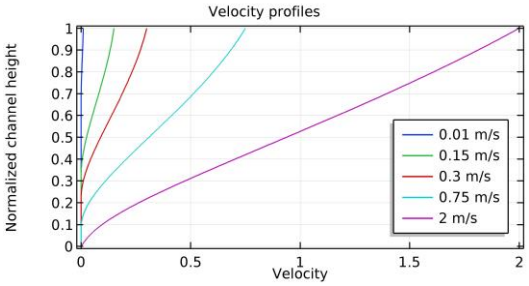

Figure 5-9: Flow velocity over the height of the channel.

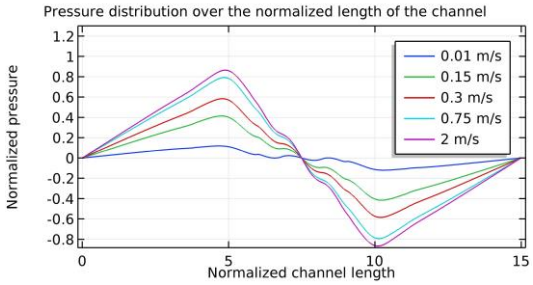

Figure 5-10: Pressure over the length of the bearing for different translational speeds.

As a next step, the goal was set to find some experimental validations of these models. These experiments eventually resulted in the discovery of the so-called "self-healing" behaviour that such a bearing configuration can adopt. Chapter 8 contains a summary of the work performed on this subject.

6 Rheological textures in journal bearings

"We do not believe it will ever be a commercial vehicle at all. We do not believe it will find any very large place in the world of sport. We do not believe its military importance is as great as commonly supposed, or will extend (except accidentally) beyond the range of scouting and courier service."

— "The Value of the Aeroplane", The Engineering Magazine, Nov 1909

This chapter contains the highlights of the work presented in A12 and [87]. See these sources for more background on the different topics discussed in this chapter.

The concept of rheological textures led to the invention of a multitude of new bearing configurations [87]. We have selected to focus on studying the characteristics of the bearing configurations presented in Figure 6-1 and Figure 6-2. The first figure presents the unfolded geometry of a hydrostatic journal bearing configuration with three bearing pads formed using rheological textures. The second figure presents a hydrodynamic journal bearing with rheological textures in a herringbone like geometry. The model assumes constant rheological properties across the height of the channel. With the use of the method to be presented in chapter 7, it is now possible to efficiently model the behaviour of these new different bearing configurations. The rheological measurements presented in Figure 9-2 and Figure 9-1 provide the values for a realistic fluid model in the analysis. Appendix A12 holds a more extensive discussion on the methods used for achieving these results.

In the analysis, the rheological textures and pressure supplies are turned on and off to determine both the hydrostatic and the hydrodynamic pressure with and without rheological textures. This makes a direct comparison between different bearing configurations possible. Figure 6-3 a, c and d present the different configurations that are realised with the structure presented in Figure 6-1. Figure 6-3 b presents a reference configuration that is the alternative to Figure 6-3 d but now with physical textures. Figure 6-4 presents the different modelling results of the hydrodynamic, hybrid and hydrodynamic journal bearings. The next sections discuss the results from these models first individually and then generally.

The pressure distribution of Figure 6-4.a presents the results for a conventional journal bearing. A high-pressure region is located in the converging wedge of the bearing and a low-pressure region is located in the diverging wedge of the bearing. A slight change in the pressure distribution can be observed at the central pressure supply caused by a local change in film thickness.

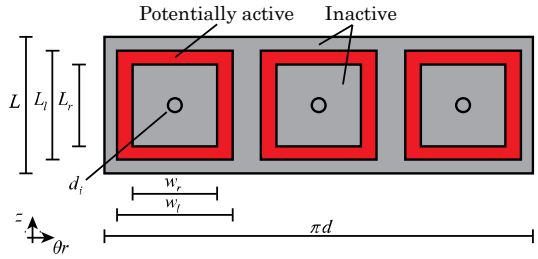

Figure 6-1: Hydrostatic journal bearing with rheological textures. (see appendix A13 for symbols)

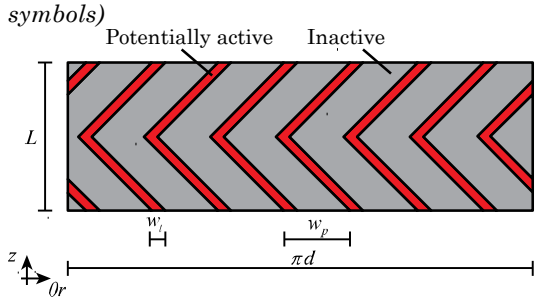

Figure 6-2: Hydrodynamic bearings design with rheological textures. (see appendix A13 for symbols)

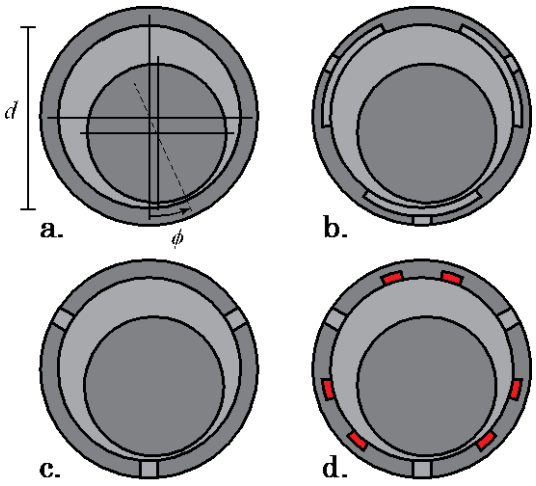

Figure 6-3: Bearing design with geometrical textures and with rheological textures.

The pressure distribution of Figure 6-4.b relates to the results of the conventional hybrid journal bearing. There is a high-pressure field located at the converging part of the bearing where there is a high pressure inlet. At the diverging part of the bearing there is a low pressure field. The results show that the pressure supply increases both the low-pressure and the high-pressure region compared to the conventional hydrodynamic bearing in Figure 6-4.a. In practise this results in less cavitation in the diverging part of the bearing.

The pressure distribution of the hydrodynamic bearing with rheological textures in Figure 6-4.c shows a high-pressure field at the converging part of the bearing and a low-pressure field at the diverging part of the bearing. A comparison of this pressure distribution with the one in Figure 6-4.a shows significant differences. Firstly, there is a larger magnitude in pressure compared to the conventional hydrodynamic bearing, and secondly there is a high-pressure region within the square annulus formed by the rheological texture.

Figure 6-4.d presents the situation where there is both a high-pressure lubricant supply and a rheological texture. The results show a high-pressure field within the activated square annulus at the converging wedge which is higher compared to the pressure field of the previous graph due to the high-pressure lubricant supply. This is comparable to the conventional hydrostatic journal bearing where a high-pressure field exists in the recess of the bearing. The square annulus enclosed by the rheological texture functions as a recess, the square annulus itself functions as a pad area.

Figure 6-5 presents the results of the hydrodynamic bearing configuration using a rheological texture in the shape of a herringbone. The results again show that the rheological texture changes the pressure distribution of the hydrodynamic journal bearing significantly. The texture shows an increase in pressure at the converging wedge and a decrease in pressure at the diverging wedge.

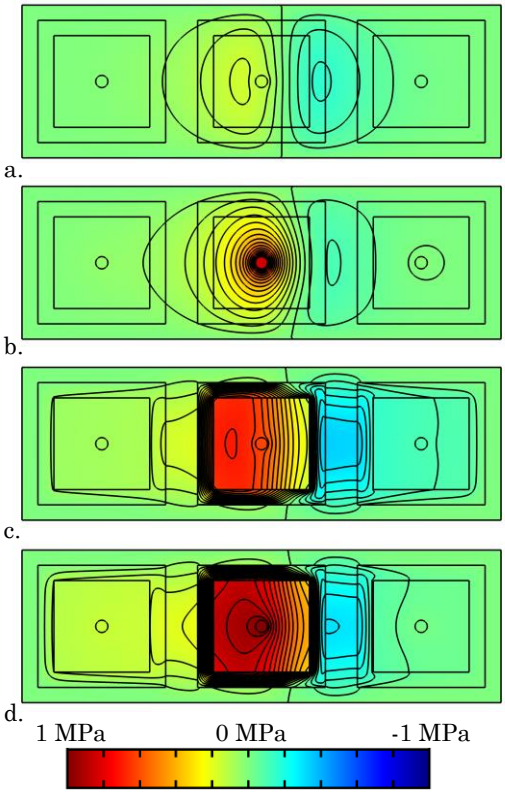

Figure 6-4: a. Pressure distribution of a conventional hydrodynamic bearing with non-activated regions. b. Pressure distribution of a conventional hybrid bearing with non-activated regions. c. Pressure distribution of a hydrodynamic bearing with activated regions. d. Pressure distribution of hybrid bearing with rheological textures.

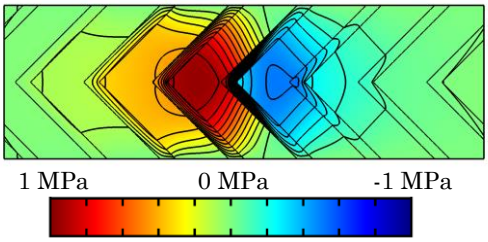

Figure 6-5: Pressure distribution of a herringbone bearing.

From the results of Figure 6-4 and Figure 6-5 it follows that the application of rheological textures causes the specific load capacity (load per area) to increase significantly for both the hydrostatic and the hydrodynamic operating conditions.

The hybrid journal bearing using a rheological texture as presented in this chapter exhibits a comparable behaviour to that of a conventional hydrostatic bearing that uses a geometrical texture. A big advantage of the rheological textures occurs when the high-pressure lubricant supply is de-activated. In this situation, a geometrical texture might result in an insufficient build-up of lubricant film, causing the two bearing surfaces to touch and eventually lead to wear. This is not the case when using a rheological texture since the bearing operates as a hydrodynamic bearing with a rheological texture where there is no actual geometrical texture susceptible to wear.

Normally, the design of a hybrid bearing implies that both hydrostatic and hydrodynamic working regimes are compromised. Surface textures needed for a proper hydrostatic operation reduce the hydrodynamic operation and vice versa. The use of rheological texture avoids this drawback. Textures can be made that only affect the local flow resistance and do not affect the local lubricant transportation rate.

The research shows that the bearing performance can be enhanced by using rheological textures. This principle adds an extra parameter in the design of a bearing that can be used to boost the performance.

7 A lubrication theory for Bingham plastics

"Failure is the condiment that gives success its flavour."

— Truman Capote, 1972

This chapter contains the highlights of the work presented in appendix A14. See these appendices for more background on the different topics discussed in this chapter.

Chapter 6 discussed some more complex bearing designs using rheological textures compared to the designs of chapter 5. The rheological behaviour of magnetorheological fluids is accurately described using the Bingham plastic fluid model, which exhibits a solid-state behaviour below a limiting shear stress, and Newtonian fluid behaviour above this shear stress. This chapter discusses the newly derived lubrication theory for Bingham plastics, used to compute the performance of rheological textured bearing designs in an efficient way. This is especially important, for example, for an engineer that needs to design a bearing system according to desired specifications and needs to compare different bearing designs in a convenient way.

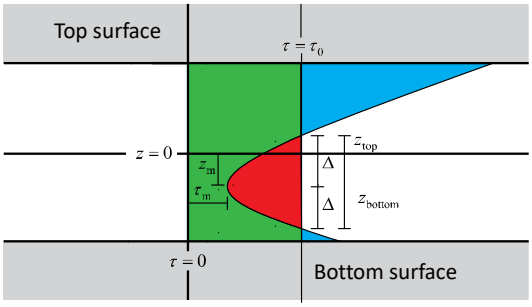

Figure 7-1: Example of a stress magnitude in the lubricating film. The green surface presents the yield stress of the fluid that should be overcome to cause flow. The red surface presents the lack of stress present to cause a flow (plug area) and the blue surface presents the stress that can cause flow. (see appendix A14 for symbols and a more detailed explanation of the figure)

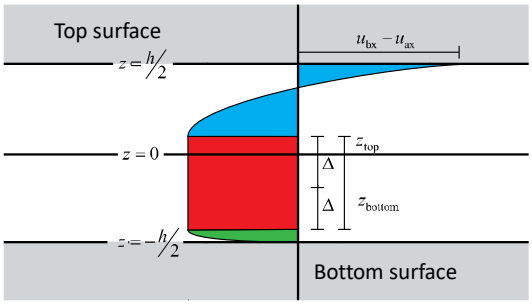

Figure 7-2: Example of the velocity profile within a lubricating film. The red part behaves as a solid plug and the green and blue part behave as a liquid. (see appendix A14 for symbols and a more detailed explanation of the figure)

The big challenge in modelling the flow of the lubricant is to properly accommodate for the yield stress in the fluid. Figure 7-1 presents an example of the total stress between the bearing faces, together with the yield stress level. The red part in between these curves indicates the stress that is lacking to cause a flow (plug area) since the stress there is lower than the yield stress. The blue part indicates the stress that is available to create flow since the stress there is higher than the yield stress. Figure 7-2 presents the corresponding flow profile that is then present in the lubricating film. The figure shows that in the red part of the channel, the lubricant behaves as a solid and at the edges, the fluid behaves as a liquid.

Literature describes three methods to model this in a 2D lubricating film. The first method is to use the full 3D (Navier-)Stokes relations together with a CFD simulation to model the flow in the full 3D extend of the lubricating film [135], [144], [162]–[165]. The second method is to use the approximated thin film model presented by Wada et al. [143], [151], [166]–[168]. The third method is to use the regularization technique used by Dorier and Tichy [154]. An additional fourth method from Tichy [153] exists which is an exact lubrication theory that is applicable to a 1D lubricating film [148], [169]. An exact lubrication theory, in which no additional approximations are required to deal with non-linearity due to the yield stress and that is applicable to a 2D lubricating film, was lacking in literature.

Therefore, in this research an exact lubrication theory for a Bingham plastic fluid has been developed. The theory is said to be exact in the sense that it requires no additional approximations than the ones already used in the Generalized Reynolds Equation [170]. The method is tested against other results presented in literature. Simulations on both infinite and finite journal bearings are performed.

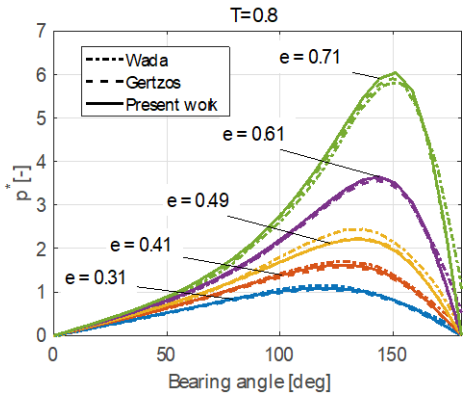

Figure 7-3: Pressure as a function of the bearing angle (or circumferential position) for the present study and some results from literature.

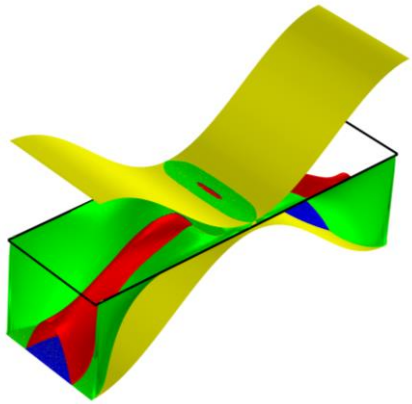

Figure 7-4: Example of the shape of the plug due to the yield stress in the fluid. The volume enclosed blue and red surfaces defines the plug.

The modelling method to describe the flow of the Bingham plastic in a thin film flow is similar to the conventional Reynolds equation. In this method too, a relation exists that describes the flow rate between the bearing surfaces as a function of the pressure gradients, surface speeds and geometry of the system. The system is finally solved in a set of nonlinear second order partial differential equations. More details on the method and on the derivation is presented in Appendix A14.

Figure 7-3 shows a comparison of the results generated with this new method and the results taken from literature. The graph presents the pressure distribution along the lubricating film of a hydrodynamic journal bearing lubricated with a Bingham plastic. The results demonstrate that the different methods are in close correspondence. Figure 7-4 shows an example of the shape of the solid-state plug formed in a hydrodynamic journal bearing. The yellow surfaces present the top and bottom surfaces, the blue surface presents the bottom of the plug, the red surface presents the top of the plug and the green surface presents the location where no plug is present (since it presents the locations of minimum shear stress that are lower than the yield stress) . The surfaces show that the resulting solution from the method is very smooth.

The results on the hydrodynamic journal bearing lubricated with a Bingham plastic fluid demonstrate that the new method is able to accurately model the bearing behaviour. One big advantage of the method is that it does not approximate the Bingham model anymore but has an exact implementation of the material model. Another big advantage is that it is computationally more efficient than other existing modelling methods. This is especially beneficial for engineering purposes.

8 Self-healing bearings

Truth is stranger than fiction, but it is because fiction is obliged to stick to possibilities; truth isn't.

— Mark Twain, 1897

This chapter contains the highlights of the work presented in appendix A15 and [88]. See these references for more background on the different topics discussed in this chapter.

During this research project we studied hydrostatic thrust bearings using rheological textures in which a strong magnetic field gradient across the film is present (chapter 5). The drawing in Figure 8-1 presents the design of a hydrodynamic thrust bearing and Figure 8-2 presents three different manufactured bearing surfaces. These surfaces have magnets at angles of $\theta = 0°$, $\theta = 30°$ and $\theta = 36°$ to be able to do measurements at different load capacities.

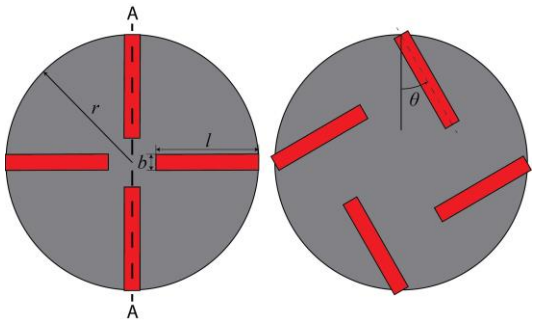

Figure 8-1: Drawing of the hydrodynamic bearing designs used to show the self-healing bearing principle. The angle θ indicates the angle of all four magnets.

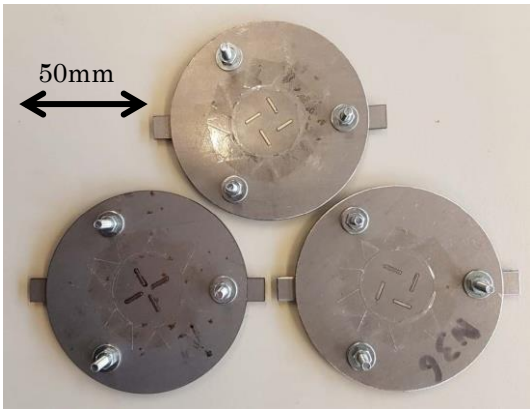

Figure 8-2: Picture of the hydrodynamic bearing designs used to show the self-healing bearing principle.

During measurements, results were not matching the expectations from the numerical model as presented in chapter 5. A load carrying capacity was measured, but both the magnitude and the shape of the pressure distribution were not as expected. After the experiment, all the particles appeared to be out of suspension and near the magnets such that only a clear carrier fluid remained. The hypothesis here was that the gradient in the magnetic field pulled the particles from suspension, creating small geometrical textures that create a pressure field that in turn creates a load capacity (see appendix A15 for more graphical material on this).

Figure 8-3 shows the load capacity as a function of the rotational speed of the bearing for both the perfectly mixed lubricant (rheological texture from chapter 4 and 5) and the lubricant with complete sedimentation near the magnets (geometrical texture). The three different graphs present three different magnet configurations. Figure 8-4 presents the measurements of the load capacity as a function of the rotational speed of the different bearing systems with complete sedimentation. The data shows that there is a close agreement between the measurements and the model that considers complete sedimentation of the particles.

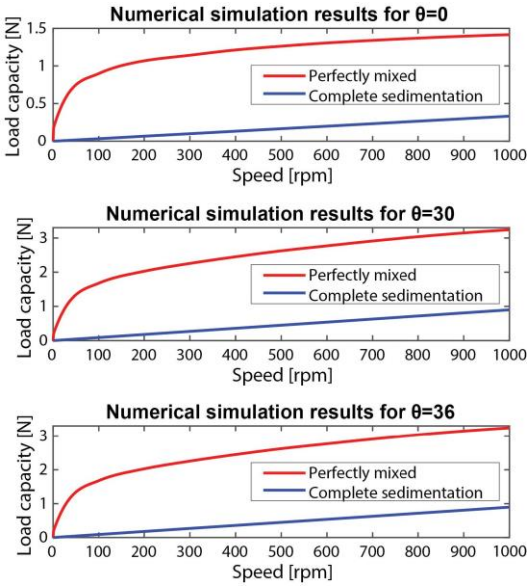

Figure 8-3: Load vs. speed. Red line: rheological textures, blue line: self-healing concept.

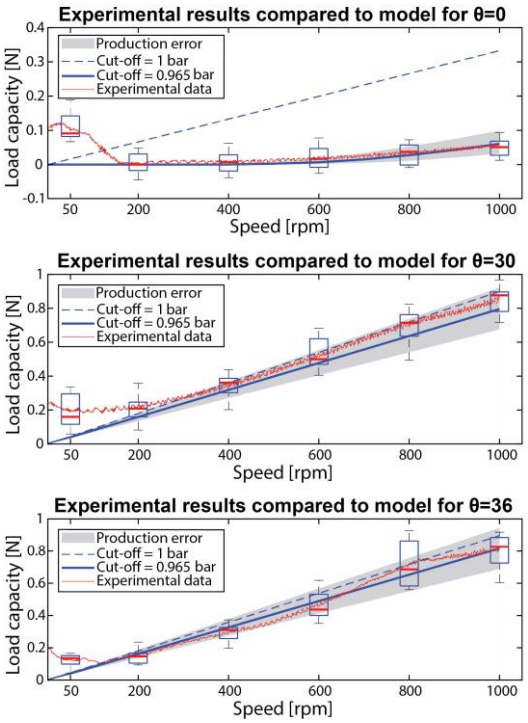

Figure 8-4: Load capacity as a function of the rotational speed for the self-healing bearing concept.

The performed experiments partially validate the hypothesis that a local gradient in the magnetic field can be large enough to pull particles out of suspension and create a local texture that creates a load carrying capacity. When this texture wears off again, the particles go back into suspension. The particles that are in suspension can settle near another texture and thus that one grows bigger. This creates a concept in which textures that wear, simply heal themselves back again, a self-healing texture. Figure 8-5 and Figure 8-6 give a graphical representation of this process. To our knowledge, this process has not been presented before. Based on this working concept, a patent has been filed specifying a multitude of new bearing designs derived from this working concept. [88] contains more information on the various designs possible.

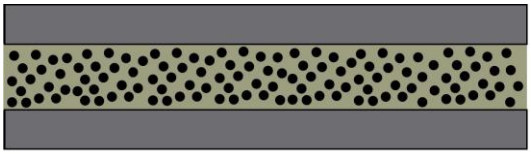

Figure 8-5: MR fluid without magnets present.

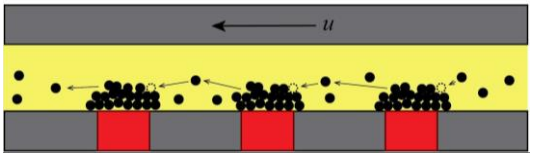

Figure 8-6: MR fluid where all the particles gather near the magnets.

The geometric surface texture of bearing systems has recently been discussed extensively in the tribological community [171]–[180]. One of the drawbacks of these textures is that they are relatively sensitive to wear. A hot topic in the scientific literature currently is to solve the limited lifetime of systems by making the materials self-healing [181]–[187]. The concept proposed in this chapter adds another solution to this field applicable to bearing systems. In addition, the shape of the textures can be reconfigured during operation by changing the magnetic field.

To further develop this concept, a large scale test setup is currently being designed that has as a goal to validate both the self-healing bearing concept and the concept of rheological textures. The setup has a 200mm shaft such that the textures can be realized with a larger relative precision in a convenient way. See the draft paper in appendix A15 or the patent application in [88] for more information on this concept.

9 Rheological characterization of magnetic fluids

"What does not kill me makes me stronger."

— Friedrich Nietzsche, 1888

This chapter contains the highlights of the work presented in appendix A16. See this appendix for more background on the different topics discussed in this chapter.

During the experimental work on the bearing systems, it became evident that both the change in yield stress and the change in viscosity of the lubricant as a function of the magnetic field are of major importance to the behaviour of the system. Figure 9-2 and Figure 9-1 together demonstrate that the properties change significantly as a function of the magnetic field strength. This change in rheological behaviour is caused by the development of chains of magnetic particles in the fluid aligned with the magnetic field [188], [189]. Also the anisotropy of the rheology is an important factor to consider [130], [190]–[195]. Since we use the fluid rheology in this thesis only for situations where the magnetic field is perpendicular to the flow, it is not covered here but it is recommended as future research. Literature generally focusses on the effect on the yield stress, and less on the effect on the viscosity of the magnetorheological lubricant. To gain more knowledge on the rheological behaviour of magnetorheological fluids under the

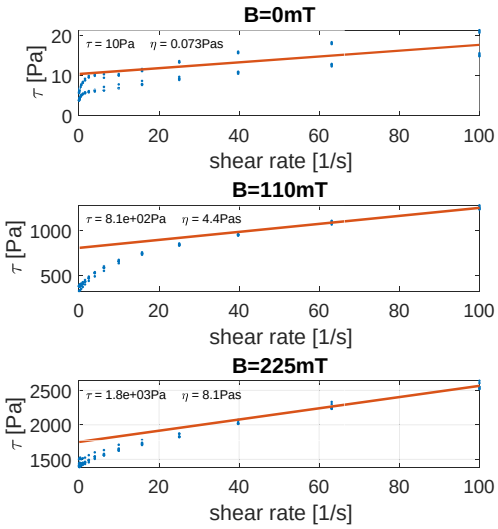

Figure 9-2: Yield stress of the magnetorheological fluid from appendix A11 as a function of the shear rate under different magnetic field strengths. The solid line presents a fit to the Bingham model.

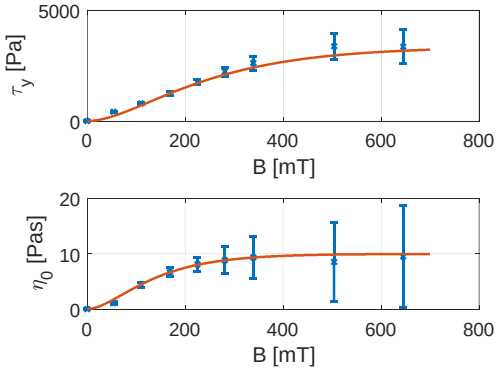

Figure 9-1: Bingham model fit of the yield stress and viscosity as a function of the magnetic field strength. Magnetorheological fluid taken from appendix A11.

conditions present in a bearing system, a new type of magnetorheometer has been developed. In this magnetorheometer rheological properties at high shear rates can be determined, which are particularly relevant for bearing applications.

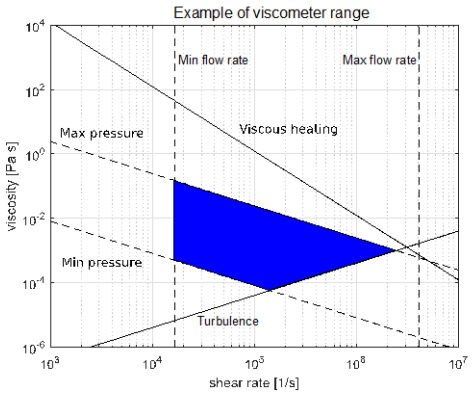

Figure 9-3: Effective viscosity as a function of the shear rate. The blue surface presents the operation range of the measurement device.

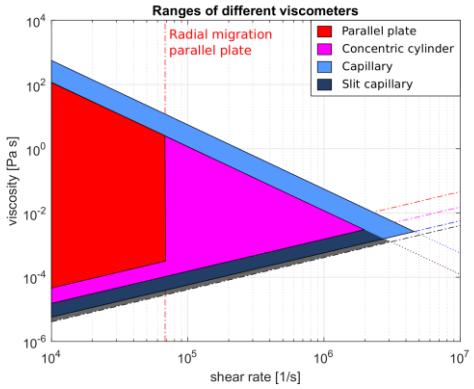

Figure 9-4: ranges of different viscometer devices. Note that the different envelopes are overlapping.

The currently available commercial rheometers that are able to characterise magnetic fluids are only able to measure the fluids at relatively low shear rates compared to those found in bearing systems [196]–[202]. For this reason, a project was started to focus on the development of a magnetorheometer that is able to characterize magnetic fluids at high shear rates.

Different types of rheometer concepts exist, all with their advantages and disadvantages [203]–[205]. Figure 9-3 presents in a graphical way the most important physical limitations of different rheometers. Those limitations define a certain envelope for the operational range of the device. Figure 9-4 displays these limitations for different rheometer concepts with similar dimensions, note that the different envelopes lay on top of each other. The figure demonstrates that the capillary rheometer is able to achieve the highest shear rates and the parallel plate rheometer performs the worst at achieving high shear rates. The commercially available rheometers that are able to characterise magnetic fluids are parallel-plate or cone-plate devices and are therefore not desired for characterizing fluids at high shear rates [200]–[202].

Based on the results of Figure 9-4 the project focuses on building a demonstrator of a microcapillary rheometer that is able to measure magnetorheological fluids at high shear rates. Figure 9-5 and Figure 9-6 shows the capillary device and the magnetic field generator. The capillary device is basically a microfluidic device in which the fluid sample flows through a narrow channel in which the pressure drop is measured. The device therefore has four connection points: a fluid inlet, a fluid outlet, a high pressure measuring channel and a low pressure measuring channel. Across the capillary device, there is a magnetic field generator that controls the amount of magnetic field through the sample during the measurement using an electromagnet. The direction of the field is perpendicular to the channel.

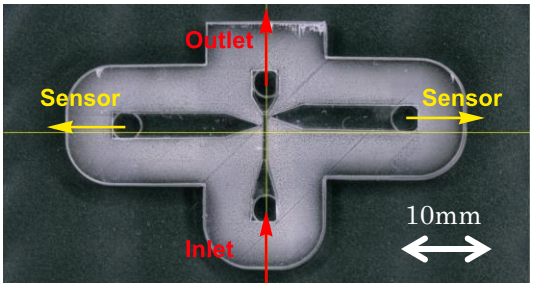

Figure 9-5: Microcapillary device containing a flow channel and two sensor outlets. The field is perpendicular to the picture.

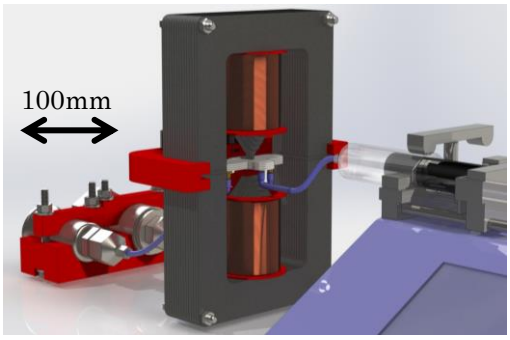

Figure 9-6: Total system overview. The magnetic field generator is located in the middle.

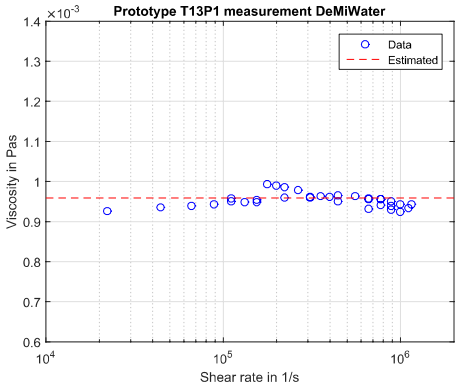

Figure 9-7: Effective viscosity as a function of the shear rate for demineralized water.

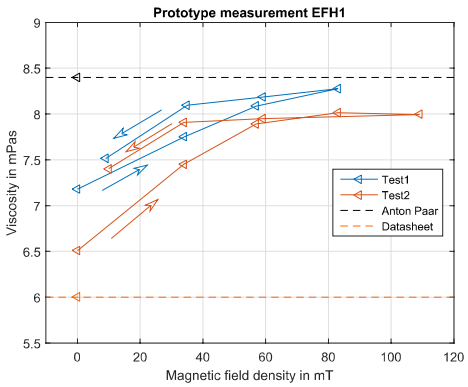

Figure 9-8: Effective viscosity as a function of the magnetic field strength for the EFH1 ferrofluid from Ferrotec.

Figure 9-7 shows a measurement on purified water to validate the accuracy of the microcapillary device and its ability to measure up to a shear rate of $1.16 \times 10^6 s^{-1}$. Figure 9-8 shows the rheology measurement of the ferrofluid EFH1 from Ferrotec [206] as a function of the magnetic field strength with a constant shear rate of $1.8 \times 10^4 s^{-1}$. The graph shows the value from the datasheet, the measurements form a commercially available rheometer and the measurement from the current microcapillary device. All data are relatively close to each other. This shows that is it possible to produce a capillary rheometer that is able to characterize the rheology of magnetic fluids at high shear rates. Appendix A16 contains a more extensive discussion on the magnetorheometer in this chapter.

10 Conclusions

Don't worry about people stealing an idea. If it's original, you will have to ram it down their throats.

As quoted, without citation, in Robert Slater, Portraits in Silicon (1987). Howard H. Aiken in reply to a student expressing concern that his own ideas might be stolen before he had published his own thesis.

This chapter gathers all the main conclusions of the six focus areas within this research. The ambition we had within the thesis project was to develop technology that could eventually serve society. To indicate the technology matureness of the different focus areas we use the Technology Readiness Level (TRL) scale as defined in [207] and presented in Table 10-1.

10.1 Ferrofluid bearings

Ferrofluid bearings are interesting due to their pure viscous friction and simplicity. At the start of the project, little knowledge existed on how to make a certain design according to specifications. So, within this project the goal became to develop the necessary knowledge to design a ferrofluid bearing according to desired specifications.

The main contributions of this thesis on ferrofluid bearing design are as follows:

- This is to our knowledge the first significant work on the modelling of ferrofluid pocket bearings.
- The work provides different experimentally validated models for the load capacity, torque capacity, out of plane stiffness, rotational stiffness, friction and operational range for both ferrofluid pocket bearings and ferrofluid pressure bearings.
- The models provide the most important bearing parameters with relevant accuracy for engineering purposes. This allows the user to design a bearing system according to a desired set of specifications.
- The different bearing systems that have been designed, built, and tested show that ferrofluid bearings can be used in a linear guidance to make long stokes.
- The latest demonstrator shows to have specifications that are competitive with conventional bearing systems.
- The technology has been demonstrated in a relevant industrial environment which brings the technology to a TRL of 6.

10.2 Ferrofluid seals

Ferrofluid seals have proven themselves in the design of commercial machines to be a good gas/gas seal due to their near zero leakage, low friction and long lifetime. Problem is that this is not yet true for ferrofluid seals that seal an gas/liquid interface. Multiple sources from literature show that these systems inevitably show a system failure over time. The goal of the work in this thesis on ferrofluid seals can be described as the development of a ferrofluid gas/liquid seal that has an infinite lifetime.

The main contributions of this thesis on the gas/liquid ferrofluid seals are as follows:

- The project invented the concept of replenishing the ferrofluid such that there always is fresh ferrofluid in the seal.
- Experimental results show that the replenishing system solves the seal failure. The seal system design ensures that degraded ferrofluid is removed and replaced by fresh ferrofluid. This gives the system a theoretical infinite lifetime, as long as the replenishing system is active. If a failure in the replenishing system occurs, this is easy to fix since the replenishment system is located outside the sealing system.
- Replenishing the ferrofluid has been shown to work even over multiple sealing steps. The ferrofluid flows from seal to seal without leaking the medium that it is sealing. The sealing capacity is not negatively affected by the process of replenishment.
- Similar to the ferrofluid bearing, the technology has been demonstrated in an industrial relevant environment which brings the technology to a TRL of 6.

10.3 Rheological textures

The property of magnetorheological fluids to change their rheological behaviour in response to a magnetic field make these fluids of interest for multiple applications. Within this research, we investigated the potential of using them to improve bearings systems. This eventually led to the invention of rheological textures. The goal of the research on rheological textures thus became the investigation into the potential of this new invention.

The main contributions of this thesis on rheological textures are as follows:

- During this project the concept of rheological textures was invented. This is a local change in rheological properties of the lubricant such that there is a local change in flow resistance and/or a local change in fluid transportation rate in the lubricating film.
- A local magnetic field interacting with a magnetorheological lubricant is able to generate a rheological texture in a lubricating film geometry.
- There are different methods of creating rheological textures. One can make textures in which the rheological properties of the lubricant are uniform across the height of the channel or one can make textures in which the rheological properties across the height the channel.
- Rheological textures with uniform rheological properties across the channel affect the local flow resistance and do not affect the local lubricant transportation rate.
- A rheological texture in which the rheological properties vary across the channel can affect both the local flow resistance and the local lubricant transportation rate.

- The work shows that a rheological texture behaves similar to but not the same as a geometrical surface texture. Where a change in geometrical surface textures changes both the flow resistance and lubricant transportation rate, a change in rheological surface textures might only change the local flow resistance.
- Rheological textures are able to enhance the performance of bearing systems.
- In this project various new bearing concepts based on rheological textures have been developed and described in a patent.
- We estimate the technology at a TRL of 4 given the experimental setup developed within this project and the scientific literature already existing.

10.4 Lubrication theory for Bingham plastics

Throughout this thesis, the Bingham plastic fluid model is used to model the rheological behaviour of magnetorheological fluids. The conventional computational methods to model lubrication with these types of fluids turned out to be computationally demanding and/or only approximations of the original Bingham model. Therefore, one of the goals became the development of a computationally efficient and exact method to model the performance of a Bingham plastic fluid in a thin film for engineering purposes.

The main contributions of this thesis on the lubrication theory with Bingham plastics are as follows:

- The work presents a new general Reynolds equation that models the behaviour of a Bingham plastic fluid without making any more simplifications than those normal for lubrication theory.
- The simulations with the new method show to be in close agreement with results from literature.
- The method has proven to be more computationally efficient.

10.5 Self-healing bearings

The work on the rheological textures led to the idea of the self-healing bearing concept. Experiments showed that, if the gradient of the magnetic field strength in the fluid film is high enough, the particles are pulled from suspension and sediment near the magnets. This creates geometrical textures that reform when worn away.

The main contributions of this thesis on the self-healing bearings are as follows:

- In the project the concept of self-healing geometrical textures by using a suspension of micron sized particles and a local magnetic field gradient was developed. These textures reform when worn away.
- These textures can create geometrical surface textures in bearings system to enhance their performance.
- In the project a basic theoretical model has been developed of which the results are in close agreement with the results from experiments.
- A patent is pending on the various new bearing designs. The concept of the self-healing bearing is currently in an early phase. Due to the initial experimental results, the TRL is set to 3.

10.6 Rheological characterization

In full film fluid bearings and seals fluids are used at relatively high shear rates. This is a region where the fluid properties of magnetic fluids are not well known yet. To our knowledge, there are no commercially available rheometers that can characterise these fluids at the shear rates found in full film bearing systems. Therefore, the goal was set to develop such a rheometer.

The main contribution of this thesis on rheological characterization is as follows:

- The work developed a concept for a micro capillary rheometer that is able to characterize magnetic fluids at shear rates generally found in bearing systems.

Table 10-1: Technology readiness level of the different focus areas.

	TRL								
Ferrofluid bearings	1	2	3	4	5	6	7	8	9
Ferrofluid gas/liquid seals	1	2	3	4	5	6	7	8	9
Rheological textures	1	2	3	4	5	6	7	8	9
Self-healing bearings	1	2	3	4	5	6	7	8	9
Rheological characterization	1	2	3	4	5	6	7	8	9

Legend: Before project / During project

TRL 1: basic principles observed

TRL 2: technology concept formulated

TRL 3: experimental proof of concept

TRL 4: technology validated in lab

TRL 5: technology validated in relevant environment (industrially relevant environment in the case of key enabling technologies)

TRL 6: technology demonstrated in relevant environment (industrially relevant environment in the case of key enabling technologies)

TRL 7: system prototype demonstration in operational environment

TRL 8: system complete and qualified

TRL 9: actual system proven in operational environment (competitive manufacturing in the case of key enabling technologies; or in space)

This table summarizes the TRL of the different concepts developed within this project from the moment just prior to the start of the project and now at the time of writing. The table demonstrates that the different concepts have made a significant step to commercial TRL levels.

11 Recommendations

"Because the people who are crazy enough to think they can change the world, are the ones who do."

— Rob Siltanen, 1997

In this thesis, we made a lot of progress on bearing and sealing systems using magnetic fluids. Though, the more we know, the clearer the yet unknown is defined. The different sections below present the recommendations of the different topics in this research, it uses the same structure as in the conclusions chapter.

11.1 Ferrofluid bearings

The work in this project brought the understanding of the ferrofluid bearing to a level such that the ferrofluid bearing can be designed according to desired specifications. A demonstrator has been built that shows that the performance can be made similar to that of conventional precise positioning bearing systems. Still, there is room for improvement in the bearing system. The technology is currently relatively immature compared to conventional systems, so there is a lot of potential to boost the performance even further.

One of the promising topics to focus on in the future is the friction behaviour of the bearing. Making a translational motion with a ferrofluid bearing leaves behind a trail of ferrofluid that affects the fly height of the bearing. Using the knowledge developed in this research, a proper design can be made that keeps this effect within specifications. However, further development of this aspect of the ferrofluid bearing is recommended.

Another promising development topic is the addition of an actuator system to the ferrofluid long stroke stage. In this research program we already demonstrated that the magnet used for the ferrofluid bearing can also be used for Lorentz actuation. For now, this was only shown for relatively short strokes. Precise positioning stages in industry often have the bearing and actuation system integrated into the product, the same can be done here.

11.2 Ferrofluid seals

The replenishing concept developed within this project generates a sealing solution that has a theoretical infinite lifetime. Still, there is room for improvement. For instance, it is currently unclear what exactly is causing the degradation of the ferrofluid seal. It may be degradation of the fluid or diffusion of the ferrofluid out of the seal. Generating more knowledge on this subject will give more insight in which refresh rate is sufficient to guarantee infinite lifetime.

Another thing that is still unclear is the reduction of sealing capacity in function of the rotational speed of the shaft. A better understanding of this will most probably lead to an improved seal design.

11.3 Rheological textures

The work in this project has resulted in the invention of rheological textures. Up to this moment the concept is mainly validated by computer models that are only partly validated by experimental setups. The logical next step here would be to generate more experimental data that validates the findings from the computer models up to now.

The predicted performance of the rheological textures using magnetorheological fluids is very dependent on the material model that is assumed. Currently there is not much knowledge on which material model best describes a real magnetorheological fluid. Generating more knowledge in this field leads to closer fit between the theoretical models and the experimental results. Following that, a new generation of bearings using rheological textures can be developed.

11.4 Lubrication theory for bingham plastics

This thesis provides a computational efficient general Reynolds equation to model a Bingham plastic in a thin film flow with no other approximations than the normal thin film flow approximations. An interesting next step here would be to extend the method to more complex material models with a yield stress, such as the Herschel-Bulkley model. This would give the method a closer fit to the real material behaviour of, for example, bearings with magnetorheological fluids.

11.5 Self-healing bearings

The concept of the self-healing bearing has up to now only been validated in one single case by means of a computer model and an experimental setup. The logical next step here is to generate more experimental data to validate the self-healing concept in other test setups. Also, the validation of the concept can be strengthened by the development of a more extensive theoretical model that includes the sedimentation of magnetic particles.

11.6 Rheological characterization

The work on the rheological characterization of magnetic fluids has resulted in the realisation of a capillary rheometer that is able to characterize magnetic fluids up to shear rates of $10^6 s^{-1}$. Since the device is only a first iteration of the concept, there is room for improvement. The most important improvement is to reduce measurement time. To this end, it is recommended to further improve the design such that also small volume quantities are measurable.

References

[1] R. Zijdeman and F. R. da Silva, “Life Expectancy at Birth (Total),” 2015.

[2] M. Roser, “Life Expectancy,” *Our World Data*, 2019.

[3] E. Ortiz-Ospina and M. Roser, “Happiness and Life Satisfaction,” *Our World Data*, 2019.

[4] M. Roser, “Ethnographic and Archaeological Evidence on Violent Deaths,” *Our World Data*, 2019.

[5] S. S. Perry and W. T. Tysoe, “Frontiers of fundamental tribological research,” *Tribol. Lett.*, vol. 19, no. 3, pp. 151–161, 2005.

[6] N. K. Myshkin and I. G. Goryacheva, “Tribology: Trends in the half-century development,” *J. Frict. Wear*, vol. 37, no. 6, pp. 513–516, 2016.

[7] K. Holmberg and A. Erdemir, “Influence of tribology on global energy consumption, costs and emissions,” *Friction*, vol. 5, no. 3, pp. 263–284, 2017.

[8] Grandviewresearch, “Bearings Market Size, Share & Trends Analysis Report By Product (Ball, Roller), By Application (Automotive, Agriculture, Electrical, Mining & Construction, Railway & Aerospace), And Segment Forecasts, 2019 - 2025,” 2019.

[9] Grandviewresearch, “Gaskets and Seals Market Size, Share & Trends Analysis Report By Product, By End Use, By Application (Automotive, Electrical & Electronics, Aerospace, Oil & Gas), By Region, And Segment Forecasts, 2019 - 2025,” 2019.

[10] A. Singh and S. S. Waydande, “A Review Paper on Performance analysis of Hydrodynamic Journal Bearing with Various Types of Lubricant for Pressure Distribution and Cavitation,” *Int. J. Adv. Eng. Res. Dev.*, vol. 4, no. 8, pp. 347–354, 2017.

[11] Z. Liu, Y. Wang, L. Cai, Y. Zhao, Q. Cheng, and X. Dong, “A review of hydrostatic bearing system: Researches and applications,” *Adv. Mech. Eng.*, vol. 9, no. 10, pp. 1–27, 2017.

[12] H. Cao, L. Niu, S. Xi, and X. Chen, “Mechanical model development of rolling bearing-rotor systems: A review,” *Mech. Syst. Signal Process.*, vol. 102, pp. 37–58, 2018.

[13] P. Baart, P. M. Lugt, and B. Prakash, “Review of the lubrication, sealing, and pumping mechanisms in oil- and grease-lubricated radial lip seals,” *Proc. Inst. Mech. Eng. Part J J. Eng. Tribol.*, vol. 223, no. 3, pp. 347–358, 2009.

[14] R. Flitney, *Seals and Sealing Handbook*. 2014.

[15] K. D. Ridler, A. B. Gosling, and G. M. Edge, “Linear bearing for parallel tracking arm,” U.S. Patent 4,065,188, 1977.

[16] S. Sudo, Y. Takaki, Y. Hashiguchi, and H. Nishiyama, “Magnetic Fluid Devices for Driving Micro Machines,” *JSME Int. J. Ser. B*, vol. 48, no. 3, pp. 464–470, 2005.

[17] J. M. Guldbakke and J. Hesselbach, “Development of bearings and a damper based on magnetically controllable fluids,” *J. Phys. Condens. Matter*, vol. 18, no. 38, pp. S2959–S2972, 2006.

[18] E. Uhlmann and N. Bayat, “High precision positioning with ferrofluids as an active medium,” *CIRP Ann. - Manuf. Technol.*, vol. 55, no. 1, pp. 415–418, 2006.

[19] G. Millet and A. Hubert, “Design of a 3 DOF displacement stage based on ferrofluids.,” *ACTUATORS’06*, pp. 656–659, 2006.

[20] S. van Veen, “Planar Ferrofluid Bearings for Precision Stages,” MSc thesis, Delft University of Technology, 2013.

[21] M. Café, "Nanometer precision Six Degrees of Freedom Planar Motion Stage with Ferrofluid Bearings," Delft University of Technology, 2014.
[22] B. Assadsangabi, M. H. Tee, and K. Takahata, "Ferrofluid-Assisted Levitation Mechanism for Micromotor Applications," *Transducers Eurosensors XXVII 17th Int. Conf. Solid-State Sensors, Actuators Microsystems*, pp. 2720–2723, 2013.
[23] G. Mok, "The design of a planar precision stage using cost effective optical mouse sensors," Delft University of Technology, 2015.
[24] H. Habib, "Design of a three Degrees of Freedom planar precision stage using a single Position Sensitive Detector," Delft University of Technology, 2015.
[25] K. Raj and R. J. Boulton, "Ferrofluids — Properties and applications," *Mater. Des.*, vol. 8, no. 4, pp. 233–236, Jul. 1987.
[26] K. Raj and R. Moskowitz, "Compact Ferrofluidic Electrically conducting sealed bearing," 1989.
[27] K. Raj, J. Bonvouloir, R. Moskowitz, and F. Bloom, "Long-Life Multi-Stage Ferrofluid Seals Incorporating a Ferrofluid Reservoir," US4,865,334, 1989.
[28] K. Raj and R. Moskowitz, "Commercial applications of ferrofluids," *J. Magn. Magn. Mater.*, vol. 85, no. 1–3, pp. 233–245, 1990.
[29] K. Raj, B. Moskowitz, and R. Casciari, "Advances in ferrofluid technology," *J. Magn. Magn. Mater.*, vol. 149, no. 1–2, pp. 174–180, 1995.
[30] K. Raj and A. F. Chorney, "Ferrofluid technology - An overview," *Indian J. Eng. Mater. Sci.*, vol. 5, no. December, pp. 372–389, 1998.
[31] K. Raj, *Ferrofluids: Applications*. Elsevier, 2001.
[32] A. V. Radionov, "Application of Magnetic Fluid Seals for Improving Reliability of Air Coolers," *Chem. Pet. Eng.*, vol. 51, no. 7–8, pp. 481–486, 2015.
[33] Z. Wang and D. Li, "Theoretical analysis and experimental study on loading process among stages of magnetic fluid seal," *Int. J. Appl. Electromagn. Mech.*, vol. 48, no. 1, pp. 101–110, 2015.
[34] V. Luciani, G. Bonifazi, P. Rem, and S. Serranti, "Upgrading of PVC rich wastes by magnetic density separation and hyperspectral imaging quality control," *Waste Manag.*, vol. 45, pp. 118–125, 2015.
[35] S. Serranti, V. Luciani, G. Bonifazi, B. Hu, and P. C. Rem, "An innovative recycling process to obtain pure polyethylene and polypropylene from household waste," *Waste Manag.*, vol. 35, pp. 12–20, 2015.
[36] E. J. Bakker, P. Rem, A. J. Berkhout, and L. Hartmann, "Turning Magnetic Density Separation into Green Business Using the Cyclic Innovation Model," *Open Waste Manag. J.*, vol. 3, no. 1, pp. 99–116, 2014.
[37] T. I. Volkova *et al.*, "A ferrofluid based artificial tactile sensor with magnetic field control," *J. Magn. Magn. Mater.*, vol. 431, no. July 2016, pp. 277–280, 2017.
[38] R. E. Musumeci, V. Marletta, A. Sanchez-Arcilla, and E. Foti, "A ferrofluid-based sensor to measure bottom shear stresses under currents and waves," *J. Hydraul. Res.*, vol. 56, no. 5, pp. 630–647, 2018.
[39] S. Pathak, K. Jain, Noorjahan, V. Kumar, and R. P. Pant, "Magnetic fluid based high precision temperature sensor," *IEEE Sens. J.*, vol. 17, no. 9, pp. 2670–2675, 2017.
[40] R. Olaru, a. Salceanu, D. Calarasu, and C. Cotae, "Magnetic fluid actuator," *Sensors Actuators, A Phys.*, vol. 81, no. 1, pp. 290–293, 2000.
[41] R. Olaru, C. Petrescu, and R. Hertanu, "Magnetic actuator with ferrofluid and non-magnetic disc," *Int. J. Appl. Electromagn. Mech.*, vol. 32, no. 4, pp. 267–274, 2010.
[42] R. Olaru, C. Petrescu, and R. Hertanu, "A novel double-action actuator based on ferrofluid and permanent magnets," *J. Intell. Mater. Syst. Struct.*, vol. 23, no. 14, pp. 1623–1630, 2012.
[43] R. Olaru and C. Petrescu, "Simplified Approach for Calculating the Force of a Ferrofluidic Actuator," *Rev. Roum. des Sci. Tech.*, vol. 53, no. 4, pp. 435–443, 2008.
[44] L. Mao and H. Koser, "Ferrohydrodynamic pumping in spatially traveling sinusoidally time-varying magnetic fields," *J. Magn. Magn. Mater.*, vol. 289, pp. 199–202, 2005.
[45] V. Chaudhary, Z. Wang, A. Ray, I. Sridhar, and R. V. Ramanujan, "Self pumping

magnetic cooling," *J. Phys. D. Appl. Phys.*, vol. 50, no. 3, 2017.
[46] L. J. Love, J. F. Jansen, T. E. McKnight, Y. Roh, and T. J. Phelps, "A magnetocaloric pump for microfluidic applications," *IEEE Trans. Nanobioscience*, vol. 3, no. 2, pp. 101–110, 2004.
[47] H. M. Bajaj, G. S. Birdi, and B. A. Ugale, "Application of Magneto Rheological (Mr) Fluid," *Int. J. Mech. Prod. Eng.*, vol. 02, no. February, pp. 83–87, 2014.
[48] Z. Jiang and R. E. Christenson, "A fully dynamic magneto-rheological fluid damper model," *Smart Mater. Struct.*, vol. 21, no. 6, p. 065002, 2012.
[49] S. A. Khan, A. Suresh, and N. SeethaRamaiah, "Principles, Characteristics and Applications of Magneto Rheological Fluid Damper in Flow and Shear Mode," *Procedia Mater. Sci.*, vol. 6, no. Icmpc, pp. 1547–1556, 2014.
[50] Robert Kaiser, "Process for cleaing up oil spills," US3635819A, 1972.
[51] K. N. Krishnakumar and V. Yuvaraj, "Clearing Of Oil Spills by Magnetic Separation Method," *Imp. J. Interdiscip. Res.*, vol. 3, no. 3, pp. 156–158, 2017.
[52] M. Zahn, T. A. Hatton, and S. R. Kuhrshall, "Magnetic colloid petroleum oil spill clean-up of ocean surface, depth, and shore regions," 2012.
[53] C. Nadejde, M. Neamtu, and D. Creanga, "Environment-friendly magnetic fluids for wastewater remediation - Synthesis and characterization," *Acta Phys. Pol. A*, vol. 127, no. 2, pp. 647–649, 2015.
[54] B. A. Bolto, "Magnetic particle technology for wastewater treatment," *Waste Manag.*, vol. 10, no. 1, pp. 11–21, 1990.
[55] C.-C. Yang, X.-F. Bian, and J.-F. Yang, "Enhancing the efficiency of wastewater treatment by addition of Fe-based amorphous alloy powders with H2O2 in ferrofluid," *Funct. Mater. Lett.*, vol. 7, no. 3, 2014.
[56] M. F. Casula *et al.*, "Design of water-based ferrofluids as contrast agents for magnetic resonance imaging," *J. Colloid Interface Sci.*, vol. 357, no. 1, pp. 50–55, 2011.
[57] M. F. Casula *et al.*, "Magnetic resonance imaging contrast agents based on iron oxide superparamagnetic ferrofluids," *Chem. Mater.*, vol. 22, no. 5, pp. 1739–1748, 2010.
[58] E. H. Kim, H. S. Lee, B. K. Kwak, and B. K. Kim, "Synthesis of ferrofluid with magnetic nanoparticles by sonochemical method for MRI contrast agent," *J. Magn. Magn. Mater.*, vol. 289, pp. 328–330, 2005.
[59] S. Odenbach, "Fluid mechanics aspects of magnetic drug targeting," *Biomed. Tech.*, vol. 60, no. 5, pp. 477–483, 2015.
[60] J. L. Arias, V. Gallardo, F. Linares-Molinero, and A. V. Delgado, "Preparation and characterization of carbonyl iron/poly(butylcyanoacrylate) core/shell nanoparticles," *J. Colloid Interface Sci.*, vol. 299, no. 2, pp. 599–607, 2006.
[61] C. Alexiou *et al.*, "Magnetic drug targeting - Biodistribution of the magnetic carrier and the chemotherapeutic agent mitoxantrone after locoregional cancer treatment," *J. Drug Target.*, vol. 11, no. 3, pp. 139–149, 2003.
[62] C. Alexiou *et al.*, "Cancer therapy with drug loaded magnetic nanoparticlesmagnetic drug targeting," *J. Magn. Magn. Mater.*, vol. 323, no. 10, pp. 1404–1407, 2011.
[63] P. Kheirkhah *et al.*, "Magnetic Drug Targeting: A Novel Treatment for Intramedullary Spinal Cord Tumors," *Sci. Rep.*, vol. 8, no. 1, pp. 1–9, 2018.
[64] P. M. Price, W. E. Mahmoud, A. A. Al-Ghamdi, and L. M. Bronstein, "Magnetic drug delivery: Where the field is going," *Front. Chem.*, vol. 6, no. DEC, pp. 1–7, 2018.
[65] T. Vangijzegem, D. Stanicki, and S. Laurent, "Magnetic iron oxide nanoparticles for drug delivery: applications and characteristics," *Expert Opin. Drug Deliv.*, vol. 16, no. 1, pp. 69–78, 2019.
[66] D. Chang *et al.*, "Biologically targeted magnetic hyperthermia: Potential and limitations," *Front. Pharmacol.*, vol. 9, no. AUG, 2018.
[67] M. M. Cruz *et al.*, *Nanoparticles for Magnetic Hyperthermia Chapter Outline*. Elsevier Inc., 2017.
[68] P. Das, M. Colombo, and D. Prosperi, "Recent advances in magnetic fluid hyperthermia for cancer therapy," *Colloids Surfaces B Biointerfaces*, vol. 174, no. July 2018, pp. 42–55, 2019.

[69] E. C. Abenojar, S. Wickramasinghe, J. Bas-Concepcion, and A. C. S. Samia, "Structural effects on the magnetic hyperthermia properties of iron oxide nanoparticles," *Prog. Nat. Sci. Mater. Int.*, vol. 26, no. 5, pp. 440–448, 2016.
[70] J. L. Neuringer and R. E. Rosensweig, "Ferrohydrodynamics," *Phys. Fluids*, vol. 7, no. 12, pp. 1927–1937, 1964.
[71] S. Odenbach, "Magnetic fluids," *Adv. Colloid Interface Sci.*, vol. 46, pp. 263–282, Dec. 1993.
[72] S. S. Papell, "No Title," *Space Daily*, no. 211, 1963.
[73] S. S. Papell, "Low viscosity magnetic fluids obtained by the colloidal suspension of magnetic particles," U.S. Patent 3,215,572, 1965.
[74] R. E. Rosensweig, J. N. Nestor, and R. S. Timmens, "No Title," *Br. Inst. Chem. Eng. Inst. Chem. Eng. Jt. Meet.*, p. 15, 1965.
[75] S. A. Novopashin, M. A. Serebryakova, and S. Y. Khmel, "Methods of magnetic fluid synthesis (review)," *Thermophys. Aeromechanics*, vol. 22, no. 4, pp. 397–412, 2015.
[76] J. Rabinow, "The Magnetic Fluid Clutch," *Trans. Am. Inst. Electr. Eng.*, vol. 67, no. 2, p. 1308, 1948.
[77] J. Rabinow, "Magnetic fluid torque and force transmitting device," US Patent 2 575 360, 1951.
[78] J. Rabinow, "Magnetic Fluid Shock Absorber," 1954.
[79] J. De Vicente, "Magnetorheology : a review," *Rheo-Iba*, vol. 1, pp. 1–18, 2013.
[80] M. T. López-López, A. Gómez-Ramírez, L. Rodríguez-Arco, J. D. G. Durán, L. Iskakova, and A. Zubarev, "Colloids on the frontier of ferrofluids. Rheological properties," *Langmuir*, vol. 28, no. 15, pp. 6232–6245, 2012.
[81] A. Gómez-Ramírez, M. T. López-López, J. D. G. Durán, and F. González-Caballero, "Influence of particle shape on the magnetic and magnetorheological properties of nanoparticle suspensions," *Soft Matter*, vol. 5, p. 3888, 2009.
[82] S. G. E. Lampaert, J. W. Spronck, and R. A. J. van Ostayen, "Load and stiffness of a planar ferrofluid pocket bearing," *Proc. Inst. Mech. Eng. Part J J. Eng. Tribol.*, vol. 232, no. 1, pp. 14–25, 2017.
[83] S. G. E. Lampaert, B. J. Fellinger, J. W. W. Spronck, R. A. J. A. J. van Ostayen, and R. A. J. Ostayen, "In-plane friction behaviour of a ferrofluid bearing," *Precis. Eng.*, vol. 54, no. October 2017, pp. 163–170, 2018.
[84] S. G. E. Lampaert and R. A. J. van Ostayen, "Lubrication Theory for Bingham Plastics," *J. Rheol. (N. Y. N. Y).*, vol. In review, 2019.
[85] S. M. Allebrandi, R. A. J. van Ostayen, and S. G. E. Lampaert, "Capillary rheometer for magnetic fluids," *J. Micromechanics Microengineering*, 2009.
[86] M. C. De Graaf, R. A. J. Van Ostayen, and S. G. E. Lampaert, "Rheological textures in bearing systems with parallel surfaces," in *18TH EDF - PPRIME WORKSHOP: Challenges in sliding bearing technologies for clean and low carbon energy applications*, 2019.
[87] S. G. E. Lampaert and R. A. J. van Ostayen, "Lubricated Sliding Bearing With Adjustment Of The Properties Of The Lubricant In Certain Parts Of The Bearing Gap," WO2018212657, 2018.
[88] S. G. E. Lampaert, M. C. de Graaf, and R. A. J. van Ostayen, "Self-healing bearing device using electric or magnetic fluids," P34129NL00/WHA (pending), 2019.
[89] B. J. Fellinger, "Validation of in-plane friction behaviour of a ferrofluid bearing," Delft University of Technology (MSc thesis), 2017.
[90] S. G. E. Lampaert, R. A. J. van Ostayen, and J. W. Spronck, "Precision Applications of Ferrofluid Bearings," *Microniek*, no. 2, pp. 15–19, 2018.
[91] A. S. T. Boots, L. E. E. Krijgsman, B. J. M. de Ruiter, S. G. E. Lampaert, and J. W. Spronck, "Increasing the load capacity of planar ferrofluid bearings by the addition of ferromagnetic material," *Tribol. Int.*, vol. 129, pp. 46–54, 2019.
[92] A. S. T. Boots, J. W. Spronck, R. A. J. J. van Ostayen, and S. G. E. Lampaert, "Operational range of a ferrofluid pocket bearing," *Smart Mater. Struct.*, vol. 28, p. 13, 2019.

[93] O.G.R. Potma, S. G. E. Lampaert, and R. A. J. van Ostayen, "Method for transport of Ferrofluid in a liquid contactless rotational seal," in *17th EDF – PPRIME workshop. Green sealing: Green sealing: How to combine both low leakage and low friction?*, 2018.
[94] K. van der Wal, R. A. J. van Ostayen, and S. G. E. Lampaert, "Rotary Ferrofluid Seal with Replenishing System for Sealing Liquids," 2019.
[95] S. G. E. Lampaert and R. A. J. van Ostayen, "Load and Stiffness of a Hydrostatic Bearing Lubricated with a Bingham Plastic Fluid," *J. Intell. Mater. Syst. Struct.*, 2019.
[96] S. G. E. S. G. E. Lampaert, R. A. J. van Ostayen, and R. A. J. Van Ostayen, "Experimental results on a hydrostatic bearing lubricated with a magnetorheological fluid," *Curr. Appl. Phys.*, vol. 19, no. 12, pp. 1441–1448, 2019.
[97] R. E. Rosensweig, "Buoyancy and stable levitation of a magnetic body immersed in a magnetizable fluid.," *Nature*, vol. 210, no. 5036, pp. 613–614, 1966.
[98] R. E. Rosensweig, "Bearing arrangement with magnetic fluid defining bearing pads," U.S. Patent 3,612,630, 1971.
[99] R. E. Rosensweig, "Magnetic fluid pneumatic bearings," U.S. Patent 3,734,578, 1973.
[100] R. E. Rosensweig, "Magnetic fluid seals," U.S. Patent 3,620,584, 1971.
[101] R. E. Rosensweig, "Ferrohydrodynamics." Dover Publications, Newburyport, 2013.
[102] W. Ochofiski, "Dynamic sealing with magnetic fluids," *Wear*, vol. 130, pp. 261–268, 1989.
[103] R. A. Williams and H. Malsky, "Some experiences using a ferrofluid seal against a liquid," *IEEE Trans. Magn.*, vol. 16, no. 2, pp. 379–381, 1980.
[104] J. Kurfess and H. K. Muller, "Sealing Liquids with Magnetic Liquids," *J. Magn. Magn. Mater.*, vol. 85, pp. 246–252, 1990.
[105] Y. Mitamura, T. Yano, W. Nakamura, and E. Okamoto, "A magnetic fluid seal for rotary blood pumps: Behaviors of magnetic fluids in a magnetic fluid seal," *Biomed. Mater. Eng.*, vol. 23, no. 1–2, pp. 63–74, 2013.
[106] Y. Mitamura, T. Yano, and E. Okamoto, "A magnetic fluid seal for rotary blood pumps: Image and computational analyses of behaviors of magnetic fluids," *Proc. Annu. Int. Conf. IEEE Eng. Med. Biol. Soc. EMBS*, pp. 663–666, 2013.
[107] H. Wang and S. Wang, "Effect of Seal Gap on the Seal Life When Sealing Liquids with Magnetic Fluid," vol. 31, pp. 83–88, 2016.
[108] M. Szczech and W. Horak, "Tightness testing of rotary ferromagnetic fluid seal working in water environment," *Ind. Lubr. Tribol.*, vol. 67, no. 5, pp. 455–459, 2015.
[109] H. Wang, D. Li, X. He, and Z. Li, "Performance of the ferrofluid seal with gas isolation device for sealing liquids," *Int. J. Appl. Electromagn. Mech.*, vol. 57, no. 1, pp. 107–122, 2018.
[110] Z. Szydło and M. Szczech, "Investigation of Dynamic Magnetic Fluid Seal Wear Process in Utility Water Environment," *Key Eng. Mater.*, vol. 490, pp. 143–155, 2012.
[111] L. Matuszewski and Z. Szydlo, "Life tests of a rotary single-stage magnetic-fluid seal for shipbuilding applications," *Polish Marit. Res.*, vol. 18, no. 2, pp. 51–59, 2011.
[112] L. Matuszewski, "Multi-stage magnetic-fluid seals for operating in water – life test procedure, test stand and research results Part II," *Polish Marit. Res.*, vol. 20, no. May, pp. 39–47, 2013.
[113] L. Matuszewski, "Multi-stage magnetic-fluid seals for operating in water – life test procedure, test stand and research results," *Polish Marit. Res.*, vol. 20, no. 4, pp. 39–47, 2013.
[114] L. Matuszewski, "New Designs of Centrifugal Magnetic Fluid Seals for Rotating Shafts in Marine Technology," *Polish Marit. Res.*, vol. 26, no. 2, pp. 33–46, 2019.
[115] Y. Mitamura, M. Fujiyoshi, and T. Yoshida, "A ferrofluidic seal specially designed for rotary blood pumps," *Artif. …*, vol. 20, no. 6, pp. 497–502, 1996.
[116] Z. Li, D. Li, Y. Chen, Y. Yang, and J. Yao, "Influence of Viscosity and Magnetoviscous Effect on the Performance of a Magnetic Fluid Seal in a Water Environment," *Tribol. Trans.*, vol. 61, no. 2, pp. 367–375, 2018.
[117] T. Liu, Y. Cheng, and Z. Yang, "Design optimization of seal structure for sealing liquid by magnetic fluids," *J. Magn. Magn. Mater.*, vol. 289, pp. 411–414, 2005.

[118] Y. Mitamura, H. Nakamura, E. Okamoto, R. Yozu, S. Kawada, and D. W. Kim, "Development of the Valvo pump: An axial flow pump implanted at the heart valve position," *Artif. Organs*, vol. 23, no. 6, pp. 566–571, 1999.
[119] Y. Mitamura, K. Sekine, M. Asakawa, R. Yozu, S. Kawada, and E. Okamoto, "A durable, non power consumptive, simple seal for rotary blood pumps," *ASAIO J.*, vol. 47, no. 4, pp. 392–396, 2001.
[120] K. Sekine, Y. Mitamura, S. Murabayashi, I. Nishimura, R. Yozu, and D. W. Kim, "Development of a Magnetic Fluid Shaft Seal for an Axial-Flow Blood Pump," *Artif. Organs*, vol. 27, no. 10, pp. 892–896, 2003.
[121] Y. Mitamura, S. Arioka, D. Sakota, K. Sekine, and M. Azegami, "Application of a magnetic fluid seal to rotary blood pumps.," *J. Phys. Condens. Matter*, vol. 20, no. May 2008, p. 204145, 2008.
[122] Y. Mitamura *et al.*, "Sealing Performance of a Magnetic Fluid Seal for Rotary Blood Pumps," *Artif. Organs*, vol. 33, no. 9, pp. 770–773, 2009.
[123] Y. Mitamura, S. Takahashi, S. Amari, E. Okamoto, S. Murabayashi, and I. Nishimura, "A magnetic fluid seal for rotary blood pumps: Long-term performance in liquid," *Phys. Procedia*, vol. 9, no. 2, pp. 229–233, 2010.
[124] Y. Mitamura, S. Takahashi, S. Amari, E. Okamoto, S. Murabayashi, and I. Nishimura, "A magnetic fluid seal for rotary blood pumps: Effects of seal structure on long-term performance in liquid," *J. Artif. Organs*, vol. 14, no. 1, pp. 23–30, 2011.
[125] G. W. Stachowiak and A. W. Batchelor, *Engineering Tribology*, 4th ed. Elsevier Inc., 2014.
[126] J. Popplewell, R. E. Rosensweig, and J. K. Siller, "Magnetorheology of ferrofluid composites," *J. Magn. Magn. Mater.*, vol. 149, no. 1–2, pp. 53–56, 1995.
[127] S. Genç, "SYNTHESIS AND PROPERTIES OF MAGNETORHEOLOGICAL (MR) FLUIDS," 2002.
[128] L. Rodríguez-Arco, M. T. López-López, J. D. G. Durán, A. Zubarev, and D. Chirikov, "Stability and magnetorheological behaviour of magnetic fluids based on ionic liquids," *J. Phys. Condens. Matter*, vol. 23, no. 45, p. 455101, 2011.
[129] J. Wu, L. Pei, S. Xuan, Q. Yan, and X. Gong, "Particle size dependent rheological property in magnetic fluid," *J. Magn. Magn. Mater.*, vol. 408, pp. 18–25, 2016.
[130] P. Kuzhir *et al.*, "Magnetorheological effect in the magnetic field oriented along the vorticity," *J. Rheol. (N. Y. N. Y).*, vol. 58, no. 6, pp. 1829–1853, 2014.
[131] T. C. Halsey, J. E. Martin, and D. Adolf, "Rheology of electrorheological fluids," *Phys. Rev. Lett.*, vol. 68, no. 10, pp. 1519–1522, 1992.
[132] E. C. McIntyre, "Compression of Smart Materials: Squeeze Flow of Electrorheological and Magnetorheological Fluids," 2008.
[133] R. Stanway, "Smart fluids: current and future developments," *Mater. Sci. Technol.*, vol. 20, no. 8, pp. 931–939, 2004.
[134] R. P. Reitz and Gus F Plangetis, "Bearing Apparatus Featuring Electrorheological Fluid Lubrication," US 7,980,765 B2, 2011.
[135] J. Peng and K. Zhu, "Hydrodynamic characteristics of ER journal bearings with external electric field imposed on the contractive part," *J. Intell. Mater. Syst. Struct.*, vol. 16, no. June, pp. 493–499, 2005.
[136] W. Huang and X. Wang, "Ferrofluids lubrications: a status report," *Lubr. Sci.*, vol. 28, pp. 3–26, 2016.
[137] J. Salwiński and W. Horak, "Measurement of Normal Force in Magnetorheological and Ferrofluid Lubricated Bearings," *Key Eng. Mater.*, vol. 490, pp. 25–32, 2011.
[138] D. A. Bompos, "Tribological Design of Nano / Magnetorheological Fluid Journal Bearings," 2015.
[139] X. Wang, H. Li, and G. Meng, "Rotordynamic coefficients of a controllable magnetorheological fluid lubricated floating ring bearing," *Tribol. Int.*, vol. 114, no. April, pp. 1–14, 2017.
[140] C. A. Laukiavich, M. J. Braun, and A. J. Chandy, "A comparison between the performance of ferro- and magnetorheological fluids in a hydrodynamic bearing," *Proc.*

Inst. Mech. Eng. Part J J. Eng. Tribol., vol. 228, no. 6, pp. 649–666, 2014.
[141] J. T. J. O'Neill and I. G. Pegg, "Magnetorheological Lubrication of an Internal Combustion Engine," 2013.
[142] N. Vaz *et al.*, "Experimental Investigation of Frictional Force in a Hydrodynamic Journal Bearing Lubricated with Magnetorheological Fluid," *J. Mech. Eng. Autom.*, vol. 7, no. 5, pp. 131–134, 2017.
[143] O.-O. Christidi-Loumpasefski, I. Tzifas, P. G. Nikolakopoulos, and C. A. Papadopoulos, "Dynamic analysis of rotor – bearing systems lubricated with electrorheological fluids," *Proc. Inst. Mech. Eng. Part K J. Multi-body Dyn.*, vol. 0, no. 0, pp. 1–16, 2017.
[144] J. Peng and K. Q. Zhu, "Effects of electric field on hydrodynamic characteristics of finite-length ER journal bearings," *Tribol. Int.*, vol. 39, no. 6, pp. 533–540, 2006.
[145] J. S. Basavaraja, S. C. Sharma, and S. C. Jain, "A study of misaligned electrorheological fluid lubricated hole-entry hybrid journal bearing," *Tribol. Int.*, vol. 43, no. 5–6, pp. 1059–1064, 2010.
[146] A. Bouzidane and M. Thomas, "An electrorheological hydrostatic journal bearing for controlling rotor vibration," *Comput. Struct.*, vol. 86, no. 3–5, pp. 463–472, 2008.
[147] H. Urreta, Z. Leicht, a Sanchez, a Agirre, P. Kuzhir, and G. Magnac, "Hydrodynamic bearing lubricated with magnetic fluids," *J. Phys. Conf. Ser.*, vol. 149, p. 012113, 2009.
[148] H. Urreta, Z. Leicht, A. Sanchez, A. Agirre, P. Kuzhir, and G. Magnac, "Hydrodynamic Bearing Lubricated with Magnetic Fluids," *J. Intell. Mater. Syst. Struct.*, vol. 21, no. 15, pp. 1491–1499, 2010.
[149] K. Shahrivar, A. L. Ortiz, and J. de Vicente, "A comparative study of the tribological performance of ferrofluids and magnetorheological fluids within steel–steel point contacts," *Tribol. Int.*, vol. 78, pp. 125–133, 2014.
[150] A. J. F. Bombard, F. R. Gonc¸alves, K. Shahrivar, A. L. Ortiz, and J. De Vicente, "Tribological behavior of ionic liquid-based magnetorheological fluids in steel and polymeric point contacts," *Tribol. Int.*, vol. 81, pp. 309–320, 2014.
[151] P. G. Nikolakopoulos and C. a. Papadopoulos, "Controllable Misalagned Journal Bearings, Lubricated with Smart Fluids," *J. Intell. Mater. Syst. Struct.*, vol. 8, no. 2, pp. 125–137, 1997.
[152] P. G. Nikolakopoulos and C. a. Papadopoulos, "Controllable high speed journal bearings, lubricated with electro-rheological fluids. An analytical and experimental approach," *Tribol. Int.*, vol. 31, no. 5, pp. 225–234, 1998.
[153] J. a. Tichy, "Hydrodynamic lubrication theory for the Bingham plastic flow model," *J. Rheol. (N. Y. N. Y).*, vol. 35, no. 4, p. 477, 1991.
[154] C. Dorier and J. Tichy, "Behavior of a bingham-like viscous fluid in lubrication flows," *J. Nonnewton. Fluid Mech.*, vol. 45, no. 3, pp. 291–310, 1992.
[155] O. Ashour, C. A. Rogers, and W. Kordonsky, "Magnetorheological Fluids: Materials, Characterization, and Devices," *J. Intell. Mater. Syst. Struct.*, vol. 7, no. 2, 1996.
[156] J. M. Guldbakke, C. Abel-Keilhack, and J. Hesselbach, "Magnetofluidic Bearings and Dampers J.M.," in *Colloidal magnetic fluids : basics, development and application of ferrofluids*, 2009.
[157] N. Bayat *et al.*, "Technical Applications," in *Colloidal Magnetic Fluids SE - 6*, vol. 763, S. Odenbach, Ed. Springer Berlin Heidelberg, 2009, pp. 1–72.
[158] J. Hesselbach and C. Abel-Keilhack, "Active hydrostatic bearing with magnetorheological fluid," *Proc. Eighth Int. Conf. New Actuators*, pp. 343–346, 2002.
[159] N. Moles, "Actively controllabe hydrodynamic journal bearing design using magnetorheological fluids," The University of Akron, 2015.
[160] J. Hesselbach and C. Abel-Keilhack, "Active hydrostatic bearing with magnetorheological fluid," *J. Appl. Phys.*, vol. 93, no. 10, pp. 8441–8443, 2003.
[161] T. C. Papanastasiou, "Flows of Materials with Yield," *J. Rheol. (N. Y. N. Y).*, vol. 31, no. 5, pp. 385–404, 1987.
[162] K. P. Gertzos, P. G. Nikolakopoulos, and C. A. Papadopoulos, "CFD analysis of journal bearing hydrodynamic lubrication by Bingham lubricant," *Tribol. Int.*, vol. 41, no. 12,

pp. 1190–1204, 2008.
[163] D. A. Bompos and P. G. Nikolakopoulos, “CFD simulation of magnetorheological fluid journal bearings,” *Simul. Model. Pract. Theory*, vol. 19, no. 4, pp. 1035–1060, 2011.
[164] D. A. Bompos and P. G. Nikolakopoulos, “Rotordynamic Analysis of a Shaft Using Magnetorheological and Nanomagnetorheological Fluid Journal Bearings,” *Tribol. Trans.*, vol. 59, no. 1, pp. 108–118, 2016.
[165] P. Kim, J. I. Lee, and J. Seok, “Analysis of a viscoplastic flow with field-dependent yield stress and wall slip boundary conditions for a magnetorheological (MR) fluid,” *J. Nonnewton. Fluid Mech.*, vol. 204, pp. 72–86, 2014.
[166] S. Wada, H. Hayashi, and K. Haga, “Behavior of a Bingham solid in hydrodynamic lubrication (Part 1, General Theory),” *Bull. JSME*, vol. 16, no. 92, pp. 422–431, 1973.
[167] S. Wada, H. Hayahsi, and K. Haga, “Behavior of a Bingham solid in hydrodynamic lubrication (Part 2, Application to Step Bearing),” *Bull. JSME*, vol. 16, no. 92, pp. 432–440, 1973.
[168] S. Wada, H. Hayahsi, and K. Haga, “Behavior of a Bingham Solid in Hydrodynamic Lubrication (Part 3, Application to Journal Bearing),” *Bull. JSME*, no. September, p. 1182, 1974.
[169] P. Forte, M. Paternò, and E. Rustighi, “A magnetorheological fluid damper for rotor applications,” *Int. J. Rotating Mach.*, vol. 10, no. 3, pp. 175–182, 2004.
[170] D. Dowson, “A generalized Reynolds equation for fluid-film lubrication,” *Int. J. Mech. Sci.*, vol. 4, no. 2, pp. 159–170, 1962.
[171] A. Guzek, “Optimization of Surface Texture Shapes in Hydrodynamic Contacts,” 2012.
[172] T. Ibatan, M. S. Uddin, and M. A. K. Chowdhury, “Recent development on surface texturing in enhancing tribological performance of bearing sliders,” *Surf. Coatings Technol.*, vol. 272, pp. 102–120, 2015.
[173] R. Wahl, J. Schneider, and P. Gumbsch, “Influence of the real geometry of the protrusions in micro textured surfaces on frictional behaviour,” *Tribol. Lett.*, vol. 47, no. 3, pp. 447–453, 2012.
[174] M. Wakuda, Y. Yamauchi, S. Kanzaki, and Y. Yasuda, “Effect of surface texturing on friction reduction between ceramic and steel materials under lubricated sliding contact,” *Wear*, vol. 254, no. 3–4, pp. 356–363, 2003.
[175] N. Sarang, S. Lyndon, C. Philip, and B. Ravinder, “Manufacturing of microasperities on thrust surfaces using ultraviolet photolithography,” *Winter Top. Meet.*, vol. 28, no. 859, pp. 148–153, 2003.
[176] U. Pettersson and S. Jacobson, “Friction and wear properties of micro textured DLC coated surfaces in boundary lubricated sliding,” *Tribol. Lett.*, vol. 17, no. 3, pp. 553–559, 2004.
[177] C. Shen and M. M. Khonsari, “Numerical optimization of texture shape for parallel surfaces under unidirectional and bidirectional sliding,” *Tribol. Int.*, vol. 82, no. PA, pp. 1–11, 2015.
[178] D. Gropper, T. J. Harvey, and L. Wang, “Numerical analysis and optimization of surface textures for a tilting pad thrust bearing,” *Tribol. Int.*, vol. 124, no. March, pp. 134–144, 2018.
[179] Y. Henry, J. Bouyer, and M. Fillon, “Experimental analysis of the hydrodynamic effect during start-up of fixed geometry thrust bearings,” *Tribol. Int.*, vol. 120, no. December 2017, pp. 299–308, 2018.
[180] C. Gachot, A. Rosenkranz, S. M. Hsu, and H. L. Costa, “A critical assessment of surface texturing for friction and wear improvement,” *Wear*, vol. 372–373, pp. 21–41, 2017.
[181] M. D. Bartlett, M. D. Dickey, and C. Majidi, “Self-healing materials for soft-matter machines and electronics,” *NPG Asia Mater.*, vol. 11, no. 1, pp. 19–22, 2019.
[182] D. G. Bekas, K. Tsirka, D. Baltzis, and A. S. Paipetis, “Self-healing materials: A review of advances in materials, evaluation, characterization and monitoring techniques,” *Compos. Part B Eng.*, vol. 87, pp. 92–119, 2016.
[183] R. P. Wool, “Self-healing materials: A review,” *Soft Matter*, vol. 4, no. 3, pp. 400–418, 2008.

[184] S. R. Madara, N. S. Sarath Raj, and C. P. Selvan, "Review of research and developments in self healing composite materials," *IOP Conf. Ser. Mater. Sci. Eng.*, vol. 346, no. 1, 2018.
[185] N. N. Sitnikov, I. A. Khabibullina, V. I. Mashchenko, and R. N. Rizakhanov, "Prospects of Application of Self-Healing Materials and Technologies Based on Them," *Inorg. Mater. Appl. Res.*, vol. 9, no. 5, pp. 785–793, 2018.
[186] R. V. S. P. Sanka, B. Krishnakumar, Y. Leterrier, S. Pandey, S. Rana, and V. Michaud, "Soft Self-Healing Nanocomposites," *Front. Mater.*, vol. 6, no. June, pp. 1–20, 2019.
[187] Y. Wang, D. T. Pham, and C. Ji, "Self-healing composites: A review," *Cogent Eng.*, vol. 2, no. 1, pp. 1–28, 2015.
[188] H. E. Horng, C. Hong, S. Y. Yang, and H. C. Yang, "Novel properties and applications in magnetic fluids," *J. Phys. Chem. Solids*, vol. 62, pp. 1749–1764, 2001.
[189] C.-Y. Hong, "Field-induced structural anisotropy in magnetic fluids," *J. Appl. Phys.*, vol. 85, no. 8, pp. 5962–5964, 1999.
[190] H. Wang, C. Bi, J. Kan, C. Gao, and W. Xiao, "The mechanical property of magnetorheological fluid under compression, elongation, and shearing," *J. Intell. Mater. Syst. Struct.*, vol. 22, no. 8, pp. 811–816, 2011.
[191] E. Dohmen, N. Modler, and M. Gude, "Anisotropic characterization of magnetorheological materials," *J. Magn. Magn. Mater.*, vol. 431, pp. 107–109, 2017.
[192] E. Dohmen, D. Borin, and A. Zubarev, "Magnetic field angle dependent hysteresis of a magnetorheological suspension," *J. Magn. Magn. Mater.*, vol. 443, pp. 275–280, 2017.
[193] P. Kuzhir, G. Bossis, V. Bashtovoi, and O. Volkova, "Effect of the orientation of the magnetic field on the flow of magnetorheological fluid. II. Cylindrical channel," *J. Rheol. (N. Y. N. Y).*, vol. 47, no. 6, p. 1385, 2003.
[194] P. Kuzhir, G. Bossis, and V. Bashtovoi, "Effect of the orientation of the magnetic field on the flow of a magnetorheological fluid. I. Plane channel," *J. Rheol. (N. Y. N. Y).*, vol. 47, no. 6, pp. 1373–1384, 2003.
[195] J. Takimoto, H. Takeda, Y. Masubuchi, and K. Koyama, "Stress Rectification in MR Fluids under Tilted Magnetic Field," *Int. J. Mod. Phys. B*, vol. 13, no. 14, 15 & 16, pp. 2028–2035, 1999.
[196] X. Wang and F. Gordaninejad, "Study of magnetorheological fluids at high shear rates," *Rheol. Acta*, vol. 45, no. 6, pp. 899–908, 2006.
[197] F. D. Goncalves, "Characterizing the Behavior of Magnetorheological Fluids at High Velocities and High Shear Rates," Virginia Polytechnic Institute and State University, 2005.
[198] A. C. Becnel, W. Hu, and N. M. Wereley, "Measurement of magnetorheological fluid properties at shear rates of up to 25000 s -1," *IEEE Trans. Magn.*, vol. 48, no. 11, pp. 3525–3528, 2012.
[199] H. Hezaveh, A. Fazlali, and I. Noshadi, "Synthesis, rheological properties and magnetoviscos effect of Fe2O3/paraffin ferrofluids," *J. Taiwan Inst. Chem. Eng.*, vol. 43, no. 1, pp. 159–164, 2012.
[200] Anton Paar, "Application specific accessories for additional parameter setting," 2016.
[201] Anton Paar, "The Modular Compact Rheometer Series."
[202] TA Instruments, "Discovery Hybrid Rheometers Temperature Systems and Accessories," 2014.
[203] C. W. Macosko, *Rheology: Principles, Measurements, and Applications*. John Wiley & Sons, 1994.
[204] H. P. Sdougos, S. R. Bussolari, and C. F. Dewey, "Secondary flow and turbulence in a cone-and-plate device," *J. Fluid Mech.*, vol. 138, pp. 379–404, 1984.
[205] R. W. Connelly and J. Greener, "High-Shear Viscometry with a Rotational Parallel-Disk Device," *J. Rheol. (N. Y. N. Y).*, vol. 29, no. 2, pp. 209–226, 1985.
[206] Ferrotec, "Ferrofluid data sheet EFH series," 2011.
[207] EU Commission, "HORIZON 2020 – WORK PROGRAMME 2014-2015," 2014.

Personal reflection

Your happiness on the job has very little to do with the work itself. On Dirty Jobs, I remember a very successful septic tank cleaner, a multi-millionaire, who told me the secret to his success: "I looked around to see where everyone else was headed and then I went the opposite way. Then I got good at my work. Then I began to prosper. And then one day, I realized I was passionate about other people's crap." I've heard that same basic story from welders, plumbers, carpenters, electricians, HVAC professionals, hundreds of other skilled tradesmen who followed opportunity – not passion – and prospered as a result.

Don't Follow Your Passion, Mike Rowe, 2016

Somewhere halfway through 2015, AEGIR came to the university in search of technology that could deliver them the next generation stern tube seal. The main problems of this seal are that they suffer from wear and that they discharge oil into the environment during operation. We were at that moment working of the ferrofluid pocket bearing which was basically a seal in disguise. The big advantage of this sealing concept is that it does not wear down and that is does not suffer from leakage. The idea was mentioned to explore using this seal concept in stern tube systems, which in the end lead to a PhD project. Since I was working on the modelling and design principles of ferrofluid pocket bearings, I was a convenient candidate for the position and so they asked me.

Working four years alone on one single project. One must be crazy doing something like that, absolutely nothing for me, so I thought... Though, I really liked doing my graduation project, I didn't really feel like working yet and I wanted to do a sort of technical traineeship. A PhD project seemed to be a good opportunity to follow, but only if I would do it differently.

I divided the projects into different smaller project that could be done by a student as a MSc graduation project. In this way I could recruit a group of students around such that we could do the work as a team together. The projects that were not chosen by students I took myself and I made sure that the gaps between the projects were filled up. This strategy proved to be successful looking at the scientific output of the project: 11 journal papers and 2 patents (one pending).

This project is the greatest adventure I ever experienced, it was the most exciting period of my life, I was able to work in this project with intense passion. In hindsight, I see that my initial impression of a PhD project was utterly wrong, in the same way I was utterly wrong with some of the initial assumptions in the research. It makes me think about how utterly wrong we must be with so many things we believe in right now. Think of Columbus who was convinced he found a new way to India, never knowing he found a completely new continent instead. I think this very beautifully illustrates the process of research and the need for it in society.

Acknowledgements

Together everyone achieves more. This PhD thesis is used to assess whether I am worth the title Doctor of Philosophy. This does not mean that I am the sole contributor to the results in this thesis. For the four years, I have been surrounded by a team of colleagues and students who worked very hard to generate the results presented with this document.

The first people I want to thank are the large group of MSc graduation students I worked with. In chronological order this is Olivier Potma, Bas Fellinger, Sander Allebrandi, Sem van Aefst, Marc de Graaf, Jelle Boots, Karoen van der Wal, Stefan van den Toorn, Bas Lucieer and Gerben van der Meer. I was a real pleasure seeing you develop from insecure students that didn't really knew what they were doing to professionals that confidently and proudly presented their work they were working on for over a year. The many discussions I had with you were my biggest source of education in this project.

I was also privileged to supervise different BSc student groups in their graduation project. I am very thankful for the interesting and inspiring discussions we had. This really helped me either directly or indirectly in my research. One of the papers in this thesis is written by some bachelor students who were so enthusiastic about their research that they continued it in their free time to push it to a journal paper. Laurens Krijgsman and Bram de Ruiter, it was a real honour working with such enthusiastic people as you.

Then I want to thank my fellow PhD students of the department departments for the great time we had together and for all the fascinating discussions. In particular I want to thank Joep Nijssen who I worked with closely with. The discussions we had on bearing systems really helped me in my work, especially at the moments that I became blind for other solution.

As a PhD student you are very capable in developing new theoretical knowledge, but you are generally not so capable in making experimental setups for validating those theories. For this I want to thank the (lab) support staff Patrick van Holst, Spiridon van Veldhoven, Harry Jansen, Rob Luttjeboer, Jan van Frankenhuyzen and Reinier van Antwerpen. You really helped me out with all the practical issues of experimental setups and measurement systems. With this I also want to thank Anton Lefering of the Reactor Institute Delft for doing magnetic characterization of the magnetic fluids we used. For using the workshop at the faculty I want to thank Gerard van Vliet and Rene van Ommen.

Within the project I had the privilege to cooperate with the company AEGIR Marine. I want to thank the people Ruud Muis, Hans Dekker, Robert van Herwaarden, Roy van den Nieuwendijk and Federico Quinci for the great work we did together.

The last people I want to thank are Ron van Ostayen and Jo Spronck respectively my promotor and co-promotor but also supervisors of my master thesis. I cannot describe the huge amount of knowledge and expertise you taught me. You two played a very significant role in developing me into the person I am today. Especially Ron, I cannot imagine a better daily supervisor than you. In German they say "doctor-father" to their promotor, this is exactly what you were to me at the university. I am happy that you were always there for me when there were both technical and personal issues.

Curriculum vitae

General

1991, April 4th	Born in Terneuzen

Education

2003 – 2009	**VWO**, Science and Engineering + Science and Health, Reynaertcollege
2009 – 2013	**BSc**, Mechanical Engineering, TU Delft
2011 – 2012	**Minor**, D:Dream, TU Delft Mechanical design of the electric motors of a Formula Student race car
2013 – 2015	**MSc**, Mechanical Engineering, TU Delft (cum laude) Precision and Microsystems Engineering - Mechatronic system design Topic: Magnetic fluid bearings
2016 – Present	**PhD**, Mechanical Engineering, TU Delft Precision and Microsystems Engineering - Mechatronic system design Topic: Magnetic Fluid Bearings & Seals: Methods, Design & Application

Thesis project output

Presentations at international conferences

2019	Presentation	**Bearings with rheological texturing** 18th EDF – PPRIME workshop. Challenges in sliding bearing technologies for clean and low carbon energy applications
2019	Presentation	**Hydrodynamic lubrication theory for an exact Bingham plastic fluid model.** Leeds-Lyon Symposium on Tribology 2019
2019	Poster	**Modelling a hybrid journal bearing with magnetorheological fluids using the ideal Bingham model.** International Conference on Magnetic Fluids
2019	Poster + Demo	**A ferrofluid bearing: Just like an air bearing, but different** Gas Bearing Workshop 2019
2018	Presentation	**Zero leakage and low friction with ferrofluid seals** 17th EDF – PPRIME workshop. Green sealing: Green sealing: How to combine both low leakage and low friction?
2018	Presentation	**Methods for Variable Bearing Properties using Magnetic Fluids** 45th Leeds-Lyon Symposium on Tribology "Smart Tribology Systems"
2018	Poster	**Microcapillary Magnetorheometer** 17th German Ferrofluid Workshop
2018	Demo	**Magnetic fluid bearings** 17th German Ferrofluid Workshop
2018	Presentation	**Predicting the behaviour of magnetorheological textured bearings** The 18th Nordic Symposium on Tribology - NORDTRIB 2018
2017	Presentation	**Virtual Textured Hybrid Bearings** 44rd Leeds-Lyon Symposium on Tribology Tribomotion, where Performance and Motion meet Friction
2017	Presentation	**Hydrostatic bearing with MR texturing** 16th German Ferrofluid Workshop
2017	Poster	**Hydrostatic bearing with MR texturing** 16th German Ferrofluid Workshop
2016	Presentation	**XY360 planar positioning stage with ferrofluid bearings** DSPE conference 2016, Conference on Precision Mechatronics

2016	Poster + Demo	**Modelling and design principles of planar ferrofluid bearings** DSPE conference 2016, Conference on Precision Mechatronics
2016	Presentation	**Friction and Trail Formation of a Planar Ferrofluid Bearing** 43rd Leeds-Lyon Symposium on Tribology Tribology (The Jost Report) – 50 years on
2016	Presentation	**Load and Stiffness of a Ferrofluid Pocket Bearing** The 17th Nordic Symposium on Tribology - NORDTRIB 2016
2016	Presentation	**(2+4)DOF precision motion stage with ferrofluid bearings** 2016 Spring Meeting: Precision Mechatronic System Design and Control American Society for Precision Engineers (ASPE)

Conference papers

2016	**(2+4) DOF precision motion stage with ferrofluid bearings** S. G. E. Lampaert, J. W. Spronck, R. A. J. van Ostayen	2016 Spring Meeting: Precision Mechatronic System Design and Control American Society for Precision Engineers (ASPE)
2016	**Load and Stiffness of a Ferrofluid Pocket Bearing** S. G. E. Lampaert, M. Café, R. A. J. van Ostayen, and J. W. Spronck	The 17th Nordic Symposium on Tribology - NORDTRIB 2016
2016	**XY360 planar positioning stage with ferrofluid bearings** S. G. E. Lampaert, H. Habib, J. W. Spronck	DSPE conference 2016, Conference on Precision Mechatronics
2018	**Method for transport of Ferrofluid in a liquid contactless rotational seal** O.G.R. Potma, S. G. E. Lampaert, and R. A. J. van Ostayen	17th EDF – PPRIME workshop: Green sealing: Green sealing: How to combine both low leakage and low friction?
2019	**Rheological textures in bearing systems with parallel surfaces** M.C. de Graaf, R.A.J. van Ostayen, S.G.E. Lampaert	18th EDF - PPRIME workshop: Challenges in sliding bearing technologies for clean and low carbon energy applications

Journal papers

2018	**Load and stiffness of a planar ferrofluid pocket bearing** S.G.E. Lampaert, J.W. Spronck, R.A.J. van Ostayen	Journal of Engineering Tribology
2018	**In-plane friction behaviour of a ferrofluid bearing** S.G.E. Lampaert, B.J. Fellinger, J.W. Spronck, R.A.J. van Ostayen	Precision Engineering
2019	**Increasing the load capacity of planar ferrofluid bearings by the addition of ferromagnetic material** A.S.T. Boots, L.E. Krijgsman, B.J.M. de Ruiter, S.G.E. Lampaert, J.W. Spronck	Tribology International
2019	**Operational range of a ferrofluid pocket bearing** A.S.T. Boots, R.A.J. van Ostayen, J.W. Spronck, S.G.E. Lampaert	Journal of Physics D: Applied Physics.
2019	**Capillary Rheometer for Magnetorheological Fluids** S.M. Allebrandi, R.A.J. van Ostayen, S.G.E. Lampaert	Journal of Micromechanics and Microengineering
2019	**Load and Stiffness of a Hydrostatic Bearing Lubricated with a Bingham Plastic Fluid** S.G.E. Lampaert, R.A.J. van Ostayen	Journal of Intelligent Material Systems and Structures
2019	**Hydrostatic Bearing Lubricated with a Magnetorheological Fluid** S.G.E. Lampaert, R.A.J. van Ostayen	Current Applied Physics
2019	**A Lubrication Theory for Bingham Plastics** S.G.E. Lampaert, R.A.J. van Ostayen	Tribology International
2019	**Rheological textures in a journal bearing with magnetorheological fluids** S.G.E. Lampaert, R.A.J. van Ostayen	Journal of Magnetism and Magnetic Materials
2020	**Ferrofluid Rotary Seal with Replenishment System for Sealing Liquids** K. van der Wal, R.A.J. van Ostayen, S.G.E. Lampaert	Tribology International
2020	**Design of a passive alternative for long stroke linear aerostatic stages based on ferrofluid bearings** (in review) S. van den Toorn, Jo W. Spronck, R.A.J. van Ostayen, S.G.E. Lampaert	Precision Engineering
2020	**Design considerations for ferrofluid pressure bearing pads** (in review) S. van den Toorn, Jo W. Spronck, R.A.J. van Ostayen, S.G.E. Lampaert	Results in Engineering

Patents

2018	**Lubricated Sliding Bearing With Adjustment Of The Properties Of The Lubricant In Certain Parts Of The Bearing Gap** S.G.E. Lampaert, R.A.J. van Ostayen	WO2018212657
2019	**Self-healing bearing** (patent pending) M.C. de Graaf, R.A.J. van Ostayen, S.G.E. Lampaert	nl 2023974

Awards

2017	3rd poster price	**Hydrostatic bearing with MR texturing** 16th German Ferrofluid Workshop
2016	DSPE best demonstration	**Modelling and design principles of planar ferrofluid bearings** DSPE conference 2016, Conference on Precision Mechatronics
2016	PME best poster presentation	**Modelling and design principles of planar ferrofluid bearings** PME internal poster presentation

MSc thesis students supervised

2019 - Present	**Gerben van der Meer:** Theoretical methods for self-healing bearings
2019 - Present	**Bas Lucier:** Experimental validation of self-healing bearing model
2018 - 2019	**Stefan van den Toorn:** Ferrofluid bearings for precise positioning
2017 - 2019	**Karoen van der Wall:** Ferrofluid seals to seal liquids
2017 - 2019	**Marc de Graaf:** Magnetorheological texturing in hydrodynamic bearings
2017 - 2018	**Jelle Boots:** Ferrofluid bearings for precise positioning
2016 - 2018	**Sander Allebrandi:** Microcapillary Magnetorheometer
2016 - 2017	**Olivier Potma:** Designs for rotary shaft fluid seals in an aqueous environment using ferrofluid

BSc thesis projects supervised

2019	**Magnetocaloric pump**
2018	**Motion energy harvester optimized by implementing ferrofluid**
2017	**Design, control and evaluation of a magnetorheological damper to realise constant deceleration**
2017	**Influence of a MRF on friction in hydrodynamic bearings**
2016	**A Load and Stiffness Improvement of Planar Ferrofluid Bearings**
2016	**Ferrofluid trail formation on ferrofluidphobic surfaces**

Thesis result metrics:

- 5 conference papers published
- 9 journal papers published
- 3 journal papers in review
- 1 journal papers still to be submitted
- 1 patent accepted
- 1 patent pending
- 6 MSc students supervised (2 additional still being supervised)
- 6 BSc thesis groups supervised
- 17 contributions to international conferences:
    - 11 oral presentations
    - 6 poster presentations / demonstrations
- 3 demonstrations at Exhibition/fairs
- 3 awards for presenting the research

Appendices

Below follows an overview of the different publications that followed from this project. The different papers are accessible online through the different DOI links but are also appended as part two of this thesis.

A1. Load and Stiffness of a Planar Ferrofluid Pocket Bearing (2018)

Stefan G.E. Lampaert, Jo W. Spronck, Ron A.J. van Ostayen
Proceedings of the Institution of Mechanical Engineers, Part J: Journal of Engineering Tribology, 232(1)
https://doi.org/10.1177/1350650117739200

A2. In-Plane Friction Behaviour of a Ferrofluid Bearing (2018)

Stefan G.E. Lampaert, Bas J. Fellinger, Jo W. Spronck, Ron A.J. van Ostayen,
Precision Engineering, 54(1)
https://doi.org/10.1016/j.precisioneng.2018.05.013

A3. Precision Applications of Ferrofluid Bearings (2018)

Stefan G.E. Lampaert, Ron A.J. van Ostayen, Jo W. Spronck
Microniek, (2)
https://www.dspe.nl/mikroniek/archive/

A4. Increasing the Load Capacity of Planar Ferrofluid Bearings by the Addition of Ferromagnetic Material (2019)

Adriaan S.T. Boots, Laurens E. Krijgsman, Bram J.M. de Ruiter, Stefan G.E. Lampaert, Jo W. Spronck,
Tribology International, 129(1)
https://doi.org/10.1016/j.triboint.2018.07.048

A5. Operational Range of a Ferrofluid Pocket Bearing (2019)

Adriaan S.T. Boots, Jo W. Spronck, Ron A.J. van Ostayen, Stefan G.E. Lampaert
Smart Materials and Structures, 28(11)
https://doi.org/10.1088/1361-665X/ab2b60

A6. Design of a passive alternative for long stroke linear aerostatic stages based on ferrofluid bearings (2020)

Stefan van den Toorn, Jo W. Spronck, Ron A.J. van Ostayen, Stefan G.E. Lampaert
In review at Precision Engineering

A7. Design considerations for ferrofluid pressure bearing pads

Stefan van den Toorn, Jo W. Spronck, Ron A.J. van Ostayen, Stefan G.E. Lampaert
In review at Results in Engineering

A8. Method for Transport of Ferrofluid in a Liquid Contactless Rotational Seal (2018)

Olivier G.R. Potma, Stefan G.E. Lampaert, Ron A.J. van Ostayen
17th EDF/Pprime Workshop: "Green sealing: How to combine both low leakage and low friction?"
Paris Saclay, October 4, 2018
https://doi.org/10.1016/S1350-4789(18)30397-0

A9. Ferrofluid Rotary Seal with Replenishment System for Sealing Liquids (2020)

Karoen van der Wal, Ron A.J. van Ostayen, Stefan G.E. Lampaert
Tribology International, 150
https://doi.org/10.1016/j.triboint.2020.106372

A10. Load and Stiffness of a Hydrostatic Bearing Lubricated with a Bingham Plastic Fluid (2019)

Stefan G.E. Lampaert, Ron van Ostayen
Journal of Intelligent Material Systems and Structures, 30(20)
https://doi.org/10.1177/1045389X19873426

A11. Experimental Results on a Hydrostatic Bearing Lubricated with a Magnetorheological Fluid (2019)

Stefan G.E. Lampaert, Ron A.J. van Ostayen
Current Applied Physics, 19(12)
https://doi.org/10.1016/j.cap.2019.09.004

A12. Rheological Textures in Bearing Systems with Parallel Surfaces (2019)

Maarten C. de Graaf, Ron A.J. van Ostayen, Stefan G.E. Lampaert
18th EDF/Pprime Workshop: "Challenges in Sliding Bearing Technologies for Clean and Low Carbon Energy Applications"
EDF Lab Paris-Saclay, October 10 & 11

A13. Rheological texture in a journal bearing with magnetorheological fluids (2019)

Stefan G.E. Lampaert, Federico Quinci, Ron A.J. van Ostayen
Journal of Magnetism and Magnetic Materials, 499(1)
https://doi.org/10.1016/j.jmmm.2019.166218

A14. Lubrication Theory for Bingham Plastics (2020)

Stefan G.E. Lampaert, Ron A.J. van Ostayen
Tribology International
https://doi.org/10.1016/j.triboint.2020.106160

A15. A Self-Healing Hydrodynamic Thrust Bearing Using a Magnetorheological Fluid

Maarten C. de Graaf, Ron A.J. van Ostayen, Stefan G.E. Lampaert
Paper to be finalized.

A16. Capillary Rheometer for Magnetic Fluids (2020)

Sander M. Allebrandi, Ron A.J. van Ostayen and Stefan G.E. Lampaert
Journal of Micromechanics and Microengineering, 30(1)
https://doi.org/10.1088/1361-6439/ab3f4c